Role of Delta-like-4/Notch in the Formation and Wiring of the Lymphatic Network in Zebrafish

Ilse Geudens, Robert Herpers, Karlien Hermans, Inmaculada Segura, Carmen Ruiz de Almodovar, Jeroen Bussmann, Frederik De Smet, Wouter Vandevelde, Benjamin M. Hogan, Arndt Siekmann, Filip Claes, John C. Moore, Anna Silvia Pistocchi, Sonja Loges, Massimiliano Mazzone, Giovanni Mariggi, Françoise Bruyère, Franco Cotelli, Dontscho Kerjaschki, Agnes Noël, Jean-Michel Foidart, Holger Gerhardt, Annelii Ny, Tobias Langenberg, Nathan D. Lawson, Henricus J. Duckers, Stefan Schulte-Merker, Peter Carmeliet and Mieke Dewerchin

The online version of this article, along with updated information and services, is located on the World Wide Web at:

http://atvb.ahajournals.org/content/30/9/1695

Subscriptions: Information about subscribing to Arteriosclerosis, Thrombosis, and Vascular Biology is online at
http://atvb.ahajournals.org//subscriptions/

Permissions: Permissions & Rights Desk, Lippincott Williams & Wilkins, a division of Wolters Kluwer Health, 351 West Camden Street, Baltimore, MD 21202-2436. Phone: 410-528-4050. Fax: 410-528-8550. E-mail:
journalpermissions@lww.com

Reprints: Information about reprints can be found online at
http://www.lww.com/reprints

Role of Delta-like-4/Notch in the Formation and Wiring of the Lymphatic Network in Zebrafish

Ilse Geudens, Robert Herpers, Karlien Hermans, Inmaculada Segura, Carmen Ruiz de Almodovar,
Jeroen Bussmann, Frederik De Smet, Wouter Vandevelde, Benjamin M. Hogan, Arndt Siekmann,
Filip Claes, John C. Moore, Anna Silvia Pistocchi, Sonja Loges, Massimiliano Mazzone,
Giovanni Mariggi, Françoise Bruyère, Franco Cotelli, Dontscho Kerjaschki, Agnes Noël,
Jean-Michel Foidart, Holger Gerhardt, Annelii Ny, Tobias Langenberg, Nathan D. Lawson,
Henricus J. Duckers, Stefan Schulte-Merker, Peter Carmeliet, Mieke Dewerchin

Objective—To study whether Notch signaling, which regulates cell fate decisions and vessel morphogenesis, controls lymphatic development.

Methods and Results—In zebrafish embryos, sprouts from the axial vein have lymphangiogenic potential because they give rise to the first lymphatics. Knockdown of delta-like-4 (Dll4) or its receptors Notch-1b or Notch-6 in zebrafish impaired lymphangiogenesis. Dll4/Notch silencing reduced the number of sprouts producing the string of parchordal lymphangioblasts; instead, sprouts connecting to the intersomitic vessels were formed. At a later phase, Notch silencing impaired navigation of lymphatic intersomitic vessels along their arterial templates.

Conclusion—These studies imply critical roles for Notch signaling in the formation and wiring of the lymphatic network. (*Arterioscler Thromb Vasc Biol*. 2010;30:1695-1702.)

Key Words: vascular biology ■ gene silencing ■ lymphangiogenesis ■ notch signaling ■ zebrafish

The lymphatic vasculature regulates interstitial fluid homeostasis, fat resorption, immune defense, inflammation, and metastasis.[1] In mammals, venous blood vascular endothelial cells (BECs) differentiate to lymphatic endothelial cells (LECs).[1] In response to Sox18, prospero homeobox-1 (Prox-1) induces the lymphatic transdifferentiation of venous BECs.[1,2] Additional cues must regulate lymphatic development; however, their nature remains unknown. Another outstanding question is how lymphatics become wired into a stereotyped network. Deep lymphatics regularly fasciculate with other vessels and track along arteries.[1,3] Similar to blood vessels,[4] lymphatic sprouts have tip cells with filopodia to probe guidance cues.[5] Although molecules such as vascular endothelial growth factor receptor (VEGFR)-3, VEGF-C, Neuropilin-2, and Ccbe1 regulate lymphatic migration,[1,6] the navigation of lymphatics remains poorly understood. Thus, the mechanisms and molecules underlying lymphatic development and wiring remain largely unknown.

See accompanying article on page 1682

Intriguingly, despite the venous origin of lymph vessels, several molecules involved in arterial BEC regulation also regulate lymphangiogenesis. For instance, EphrinB2, an initial marker of arterial BECs,[7,8] regulates lymphatics later in development.[1] Sox18, together with Sox7, is required for arterial differentiation and later regulates lymphatic competence.[2] This relationship between "arterial" factors and lymphangiogenesis, and the anatomical congruence between arteries and lymphatics,[8–11] prompted us to investigate whether Notch also regulates lymphatic development. Notch and its ligand delta-like-4 (Dll4) seemed intriguing candidates, given their role in vessel branching.[4] By using gene silencing methods in zebrafish, we revealed novel roles for Dll4/Notch signaling at multiple steps during early lymphangiogenesis.
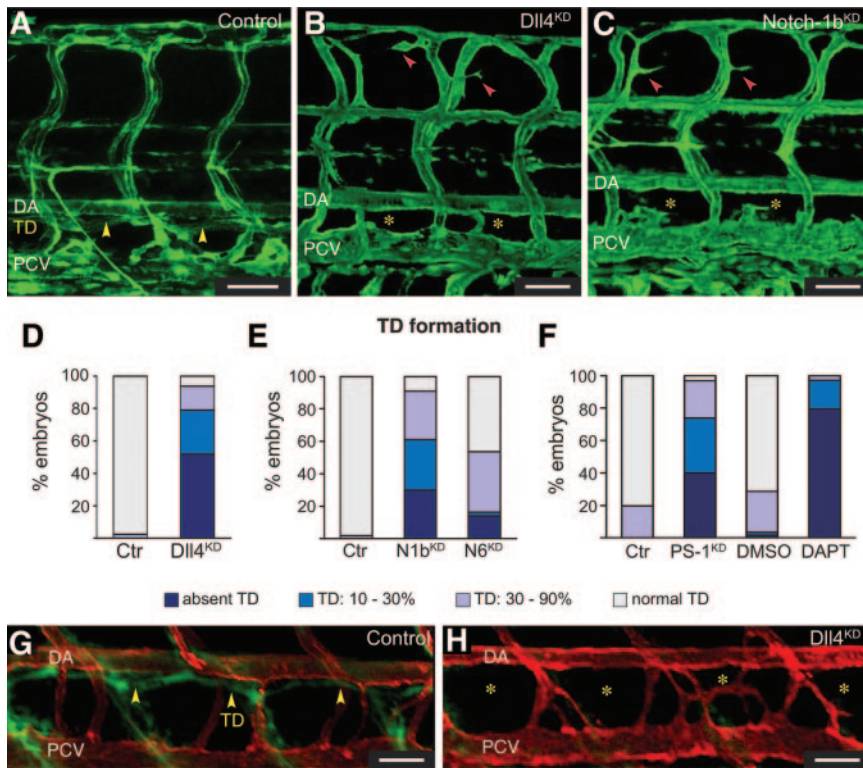
Figure 1. Role of Notch in TD formation. A through C, Confocal images of GFP⁺ vessels in *Fli1:eGFP^{y1}* embryos. Normal TD in control (yellow arrowheads; A) and absent TD in Dll4^{KD} (B) and Notch-1b^{KD} (C) embryos. Yellow asterisks indicate TD absence; red arrowheads, minimal hyperbranching of ISVs. D through F, Percentage of affected embryos in control (n=122 in D, n=185 in E, and n=87 in F) or Dll4^{KD} embryos (n=80; 10-ng Dll4^{SPL}; P<0.001; D); Notch-1b^{KD} (N1b^{KD}) embryos (n=84; 15-ng Notch-1b^{SPL}; P<0.001; E), Notch-6^{KD} (N6^{KD}) embryos (n=63; 15-ng Notch-6^{SPL}; P<0.001; E), PS-1^{KD} embryos (n=65; 2.5-ng PS-1^{ATG1}; P<0.001; F), or embryos treated with DMSO (n=171; F) or DAPT (n=34; 25-μmol/L; P<0.001; F). G and H, Lymphangiography in 7-dpf *kdr-l:mCherryRed* embryos revealed normal uptake and drainage of a green dye by the TD in the control embryo (yellow arrowheads; G), but not in the Dll4^{KD} embryo (yellow asterisks; H). The bar indicates 50 μm.

Methods

Zebrafish Husbandry

The transgenic zebrafish lines used were *Fli1:eGFP^{y1}*,[12] *Flt1:YFP*, *kdr-l:mCherryRed*, *Stab1:YFP*, *Fli1:DsRed*,[6] *Tp1bglob:eGFP*,[13] and intercrosses. Embryos and fish were grown and maintained as previously described.[6,14] All animal experimentation was approved by the institutional ethical committee.

Morpholino Injection

Morpholinos (Gene Tools, LLC, Corvallis, Ore) (supplemental Table I; all supplemental materials are available online at http://atvb.ahajournals.org) were injected at the indicated doses, as previously described.[14] Phenotyping data are pooled data from at least 3 independent experiments, with analysis of 33 to 185 injected embryos per dose. Screening methods for the evaluation of lymphatic development and functionality are detailed in the supplemental Methods.

RNA Analysis and Cell Culture Assays

Whole-mount in situ hybridization of dechorionated embryos using antisense probes for the indicated genes (supplemental Methods) was performed as previously described.[14] Quantitative RT-PCR was performed on whole embryo extracts or on fluorescence-activated cell sorted embryo cells after in vivo labeling of LECs, as described in the supplemental Methods. The proliferation, migration, and expression analyses of LECs or human umbilical venous ECs are detailed in the supplemental Methods.

Statistical Analysis

Each gene-specific morpholino was always compared with a control morpholino or vehicle. To determine the penetrance of the phenotype, we counted the number of embryos exhibiting different phenotype severities, and analyzed distributions by χ^2. Unpaired comparisons were performed by a 2-sided *t* test. Asterisks represent a significance level of *P*<0.05.

Results

Knockdown of Dll4 and Notch-1b or Notch-6 Impairs Thoracic Duct Formation

To explore a role for Notch signaling in lymphatic development (supplemental Note I and supplemental Figure I), we silenced every known zebrafish orthologue of the Notch ligands (DeltaA-D, Dll4, Jagged-1a/b, and Jagged-2) and receptors (Notch-1a/b, Notch-5, and Notch-6) and the Notch-activating presenilins-1/2 in *Fli1:eGFP^{y1}* zebrafish embryos, in which lymphatic, arterial, and venous ECs are labeled.[12,15,16] Submaximal silencing conditions were used (supplemental Note II); these conditions did not affect general or blood vascular development (supplemental Figure II and supplemental Figure III). Development of the thoracic duct (TD), the first functional lymphatic formed in the trunk in between the dorsal aorta (DA) and the posterior cardinal vein (PCV), was analyzed (supplemental Note III defines acronyms).

Dll4 morpholino knockdown (Dll4^{KD}) inhibited TD formation. On injection of a morpholino affecting Dll4 mRNA splicing (Dll4^{SPL}, 10 ng), the TD failed to form at all by 6 days post fertilization (dpf) in 52% of morphant embryos, indicating that lymphatic development was completely aborted (Figure 1A, B, and D). In another 27% of Dll4^{SPL} embryos, the TD formed over only 10% to 30% of its normal length, whereas in another 15% of morphant embryos, the TD formed over 30% to 90% of its normal length (Figure 1D). Follow-up studies at 12 dpf revealed that, in embryos with intermediate defects, the TD segments that did form failed to reconstitute the entire TD and to compensate for the lymphatic failure in nearby somites (not shown). Dll4^{KD} embryos without TD at 6 dpf also failed to form a TD, even partially, at later stages (supplemental Figure IIG and H), indicating
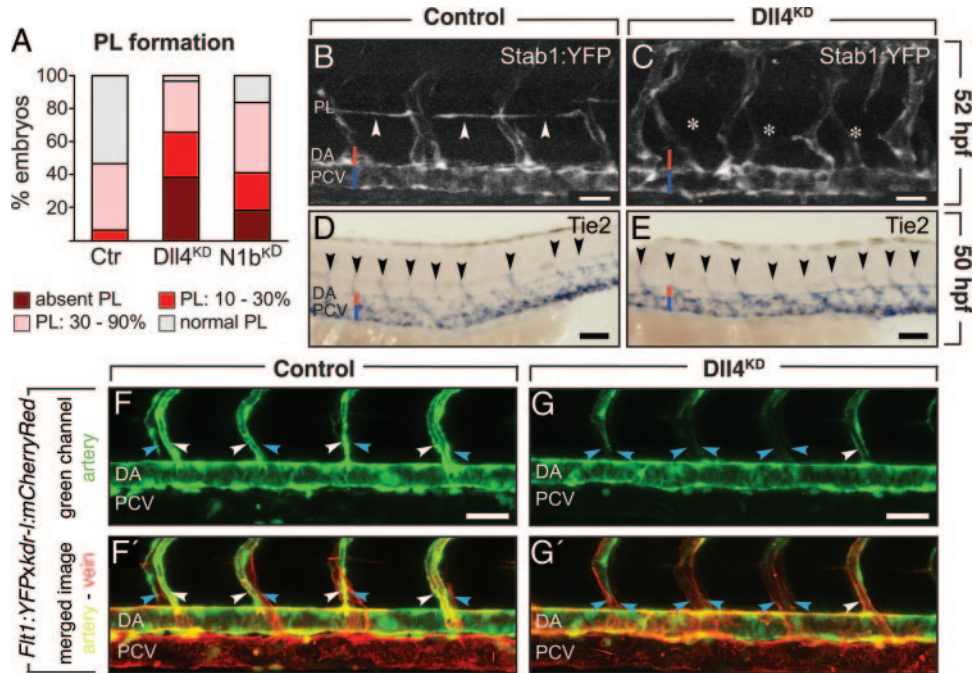
Figure 2. Silencing of Notch blocks PL and lymphangiogenic sprout formation. A, Percentage of 52-hpf embryos with affected PL in control (n=73), Dll4^{KD} embryos (n=55; 10-ng Dll4^{SPL}; $P<0.001$), or Notch-1b^{KD} embryos (N1b^{KD}) (n=49; 20-ng Notch-1b^{ATG}; $P<0.001$). B and C, Confocal images of 52-hpf *Stab1:YFP* embryos, showing normal PL in controls (arrowheads; B), but absence in Dll4^{KD} embryos (asterisks; C). D and E, Whole-mount in situ *Tie2* staining at 50 hpf, revealing normal numbers of secondary sprouts (arrowheads) in control (D) and Dll4^{KD} (E) embryos. F and G, Confocal images of vessels in *Flt1:YFPxkdr-l:mCherryRed* embryos: *kdr-l:mCherryRed* marks venous and arterial vessels red (red channel not shown), *Flt1:YFP* labels arterial vessels green (F and G), and merged images show arterial vessels yellow and venous vessels red (F'and G'). Lateral views with left and right side ISVs partially superimposed. Imaging was at 54 hpf, when secondary angiogenic sprouts had already connected to primary ISVs, which were changing arterial to venous identity in a ventral-to-dorsal pattern. In controls (F and F'), half of the aISVs became connected by angiogenic sprouts from the PCV and acquired a venous identity, thereby losing their green arterial signal (blue arrows; F) and becoming red only (blue arrows; F'), whereas the other half of the ISVs remained connected to the DA and were green (white arrows; F) or yellow in the merged image (white arrows; F'). In contrast, in the Dll4^{KD} embryo (G and G'), most ISVs lost their green arterial marker (blue arrows; G; note the single white arrow), and became marked in red only (blue arrows in G'). The white arrow in G and G' denotes a residual aISV retaining its green (G) or yellow (G') label. The bar indicates 50 μm (B, C, F, and G) or 100 μm (D and E).

that lymphatic development was not simply delayed but aborted. Similarly, incomplete silencing of Notch-1b and, to a lesser extent, Notch-6 impaired TD formation (Figure 1C and E). Of note, their mammalian orthologues, Notch-1 and Notch-2, are expressed in LECs.[10,17] Because Notch-1b downregulation causes more penetrant lymphatic defects, only data for Notch-1b^{KD} are shown.

Similar TD defects were obtained with morpholinos, targeting the ATG of Dll4 (Dll4^{ATG}) or Notch-1b (Notch-1b^{ATG}) (data not shown); however, silencing of the Notch ligands DeltaA-D, Jagged-1a/b, Jagged-2, or receptors Notch-1a, or Notch-5 (orthologue of mammalian Notch-3) did not induce lymphatic defects (data not shown). Finally, inhibition of the γ-secretase complex (which proteolytically activates Notch)[18] confirmed the involvement of Notch in lymphatic development. Both morpholino knockdown of presenilin-1 (PS-1) (but not PS-2) and pharmacological inhibition of γ-secretase activity by *N*-[N-(3,5-difluorophenacetyl)-L-alanyl]-Sphenylglycine t-butyl ester (DAPT)[18] impaired TD formation (Figure 1F, supplemental Figure IVQ and R, and supplemental Note II).

Lymphangiography in 7-dpf *kdr-l:mCherryRed* Dll4^{KD} embryos (in which only blood vessels express mCherryRed) revealed no drainage of fluorescent dye in the region in which the TD normally forms, confirming that the lack of a GFP$^+$ TD in

Fli1:eGFP^{y1} Dll4^{KD} embryos was not the result of reduced expression of GFP, but the actual absence of the vessel itself (Figure 1G and H). This assay further showed that partial TD fragments were not functional (data not shown).

Notch Is Required for Parachordal Lymphangioblast String Formation

Next, we analyzed whether silencing of Notch impaired development of the parachordal lymphangioblast (PL) cells[6] at the horizontal myoseptum because these precursors contribute to TD formation (supplemental Note I and supplemental Figure I). At 52 hours post fertilization (hpf), the formation of the PL string was completely formed in 53% and largely completed in 40% of embryos (Figure 2A). In contrast, in Dll4^{SPL} embryos, the PL string was completely absent in 38% and formed only in a few segments in 27% of embryos (Figure 2A). Largely comparable fractions of Dll4^{SPL} embryos exhibited similar types of PL string and TD defects (compare Figure 1D with Figure 2A), suggesting that the TD defects were, at least in part, attributable to defects in PL string formation. Imaging of lymphangiogenic structures in Dll4^{SPL} embryos using the *Stab1:YFP* line,[6] which primarily visualizes venous and LECs, confirmed these findings (Figure 2B and C). A similar absence of the PL string was

observed when using the Dll4^{ATG} morpholino (data not shown) or on knockdown of Notch-1b (Figure 2A) or Notch-6 (data not shown). Because the string of PL cells forms as a result of sprouting from the PCV (supplemental Note I and supplemental Figure I),[6] these findings suggest that Notch signaling acts in part at early steps.

Dll4 Silencing Reduces the Fraction of Lymphangiogenic Sprouts

Then, we studied whether inhibition of Notch acts during branching of PL-forming secondary sprouts from the PCV (termed "lymphangiogenic" secondary sprouts, denoting that they participate in the process that leads to the formation of lymphatic structures, but not blood vessels) (supplemental Note I). Whole-mount staining for *Tie2*, which marks all secondary sprouts,[19] showed a normal total number in Dll4^{KD} embryos (N=20) (Figure 2D and E). However, high-resolution imaging of 4-dpf *Fli1:eGFP^{y1}* embryos revealed alterations in the proportion of venous intersomitic vessels (vISVs) connected to the PCV. In control embryos, half of the ISVs were vISVs (percentage of total ISVs: 54±1%; mean±SEM; N=49); in contrast, in Dll4^{SPL} embryos, 82±1% of the ISVs were connected to the PCV and, thus, vISVs (mean±SEM; N=97; *P*<0.05 versus control). Similar findings were obtained in Notch-1b^{SPL} embryos (vISVs, portion of total: 69.0±2.7%; mean±SEM; N=27; *P*<0.05 versus control). Because vISVs can only be formed via connection of a secondary "angiogenic" sprout to a primary ISV (supplemental Note I), these findings, and the observation that silencing of Dll4, Notch-1b, or Notch-6 aborted PL string formation in a substantial fraction of embryos, show that a fraction of secondary sprouts that would normally have been lymphangiogenic were angiogenic, thereby impairing TD formation.

We also used high-resolution video-imaging of the double transgenic reporter line *Flt1:YFPxkdr-l:mCherryRed,*[6] labeling venous cells red (CherryRed$^+$) and arterial cells yellow (YFP$^+$CherryRed$^+$) in merged images.[6] In control embryos, half of the ISVs had a red venous color and the other half had a yellow arterial color (Figure 2F and F′). In contrast, in Dll4^{KD} embryos with severe lymphatic defects, nearly all yellow arterial ISV (aISV) connections with the DA had disappeared (single white arrow in Figure 2G and G′) (supplemental Movies I and II). Thus, a supernumerary fraction of vISV-producing angiogenic sprouts is formed in Dll4^{KD} embryos at the expense of lymphangiogenic sprouts that would otherwise proceed to form the PL string.

Dll4/Notch Promotes Lymphatic Characteristics In Vitro

To evaluate whether Notch activation in venous ECs could induce lymphatic properties, we cocultured human umbilical venous ECs, which express *Notch-1*, but negligible levels of *Prox-1* (data not shown), with monkey kidney COS cells expressing Dll4 (COS^{Dll4}) or a control vector (COS^{CTR}), and analyzed by RT-PCR with human gene-specific primers the expression of lymphatic markers. Expression levels of the lymphatic markers *PROX-1, VEGFR3, LYVE-1,* and *SOX18* in COS^{Dll4}-activated human umbilical venous ECs were moderately to distinctly elevated (Figure 3). Notably, the expression
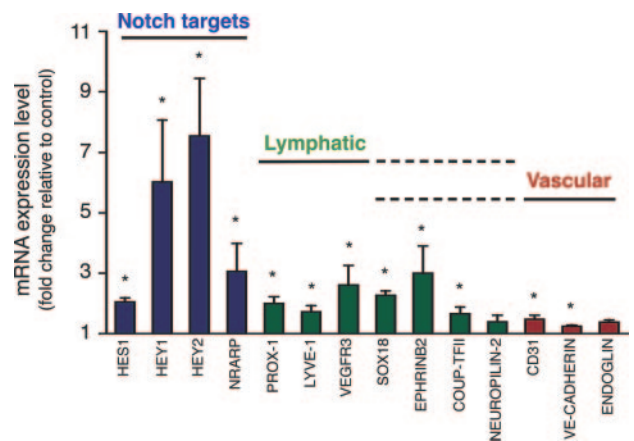

Figure 3. Notch activation by Dll4 promotes lymphatic characteristics in vitro. RT-PCR of human umbilical venous ECs (HUVECs), cocultured with COS cells expressing hDll4 (COS^{Dll4}) or control GFP (COS^{CTR}), confirming upregulation of Notch targets *HES1, HEY1, HEY2, NRARP*; blue bars) and revealing enhanced lymphatic marker expression (*PROX-1, LYVE-1, VEGFR3, SOX18, EPHRINB2*; green bars), whereas vascular genes (*CD31, VE-CADHERIN; ENDOGLIN*; red bars) were only minimally affected. *COUP-TFII* was also upregulated. *NEUROPILIN-2* was not affected. Lymphatic/arterial and lymphatic/venous genes are marked by the overlapping dashed lines. Results are fold change in HUVEC/COS^{Dll4} coculture vs HUVEC/COS^{CTR}. Data are given as mean±SEM; n=3 to 11; *P*<0.05.

levels of *EPHRINB2,* which is regulated by Notch and has been implicated in both arterial and lymphatic processes,[1,7] and *COUP-TFII,* which is expressed in both venous ECs and LECs,[20] were also upregulated; however, levels of other blood vessel markers (*ENDOGLIN, vascular endothelial [VE]-CADHERIN,* and *CD31*) were not or were only minimally affected (Figure 3). The upregulation of lymphatic markers was abolished by treatment of the cells with DAPT, 30 μmol/L (data not shown).

Silencing of Dll4 Impairs PL Cell Migration Along aISVs

From 60 hpf onward, PL cells switch to radial migration and navigate ventrally and dorsally alongside aISVs, where they form lymphatic ISVs (lISVs) (supplemental Note I). Because the TD failed to form in a fraction of Dll4^{SPL} embryos (25%) despite the presence of a partial PL string, we further explored whether Notch signaling affects lISV formation. In control embryos, lISV-PLs (PL cells that formed lISVs) migrated exclusively along aISVs, suggesting that vISVs are not permissive (Figure 4A and B). Because there were more vISVs and fewer aISVs in Dll4^{KD} embryos, migrating lISV-PLs were deprived from their arterial template and could, therefore, not contribute to TD formation (Figure 4C). This was the most common migration defect. Intriguingly, even when residual aISVs formed in Dll4^{SPL} embryos, lISV-PLs sometimes bypassed the aISV post, failing to turn and migrate along aISVs (Figure 4D). Indeed, in Dll4^{SPL} embryos with a nearly complete PL string (>90% of its length; mean±SEM; N=61), 49±6% of their aISVs were not accompanied by lISV-PLs, compared with only 15±4% in controls (mean±SEM; N=29; *P*<0.05).

Other, much less frequent, lISV defects included lISV-PLs that turned ventrally alongside the aISV but stalled (Figure 4E) or, even in a few cases, misrouted lISV-PLs
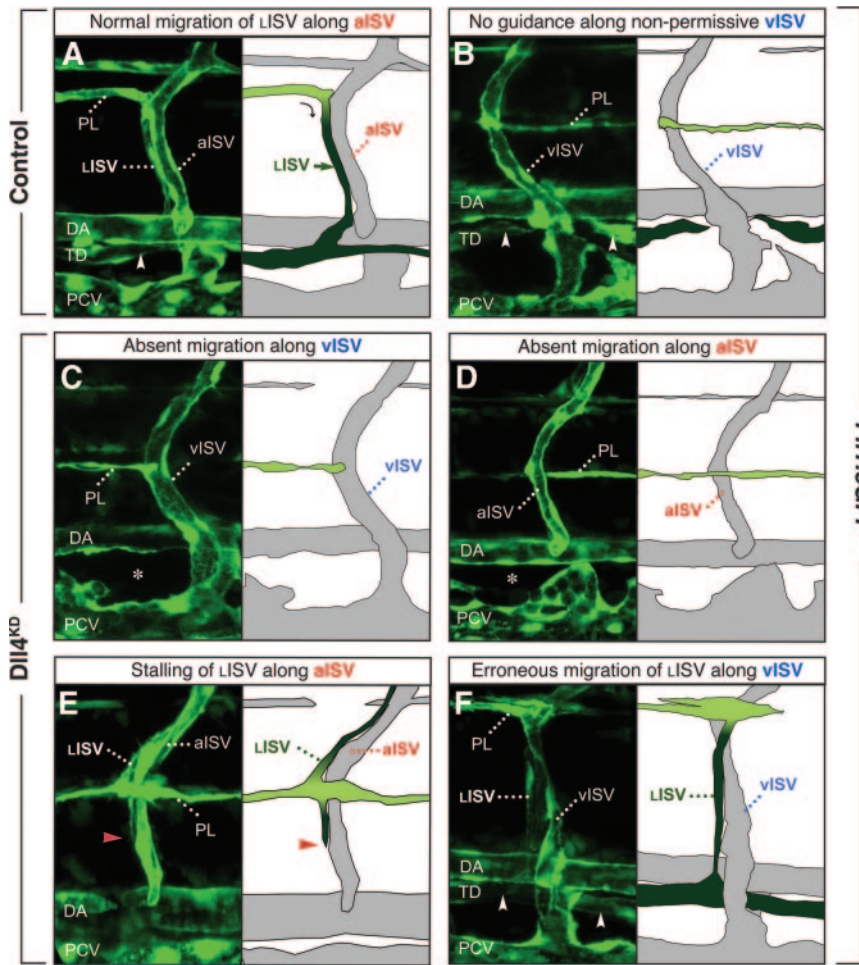
Figure 4. Incomplete silencing of Notch perturbs lymphatic navigation. Confocal images with accompanying schematic redrawing of the navigation routes of LISVs along aISVs or vISVs in 4-dpf control (A and B) and Dll4^{KD} (C-F) *Fli1:eGFP^{y1}* embryos. Permanent lymphatic structures (LISV and TD) are dark green; and transient lymphangiogenic structures (PL) are light green. A and B, In control embryos, LISV-PLs navigate alongside aISVs and establish a continuous TD (arrowhead). In A, LISVs "creep" over their aISV guidance templates; in B, LISV-PLs never navigate along vISVs in control embryos. C through F, Navigation defects in Dll4^{KD} embryos. In C, a large fraction of morphant somites, LISV-PLs, lack migration templates because fewer aISVs develop. Because LISV-PLs do not normally migrate along vISVs, no TD was formed in these somites (asterisks); in D, in other morphant somites, LISV-PLs bypassed the point of turning at the aISVs and failed to switch to radial migration; in E, in a small fraction of somites, LISV-PLs made the turn and switched to radial migration, but then stalled (red arrowhead denotes the arrested tip of a navigating LISV); and in F, in most Dll4^{KD} embryos, vISVs were not permissive to guide LISV-PLs, but, occasionally, LISV-PLs erroneously navigated alongside a vISV.

migrating along vISVs (Figure 4F). In vitro studies revealed that Notch did not regulate LEC migration/motility, proliferation, or lymphatic capillary tube formation or sprouting (supplemental Figure V and data not shown).

Expression of Dll4 and Notch

Whole-mount in situ hybridization in control embryos at 30 hpf, when secondary sprout formation starts, showed that Dll4 was detectable in the DA but not in the PCV (Figure 5A and B), in line with previous reports.[19,21,22] Notch-1b was strongly expressed in the DA (Figure 5C and D), whereas a much weaker signal appeared dispersed in certain ECs of the dorsal part of the PCV, although the low Notch-1b signal approached the detection limit of available techniques (supplemental Figure VI).

We also developed a new technique to isolate LECs from zebrafish embryos. When tetramethylrhodamine B isothiocyanate–dextran dye is injected intramuscularly in 4-week-old *Fli1:eGFP^{y1}* embryos, the red dye is taken up by LECs but not by BECs via pinocytosis, allowing fluorescence-activated cell sorting of red or green LECs. By RT-PCR, low Notch-1b transcript levels were detected in these LECs (ratio of copies of Notch-1b to 10^5 copies of β-actin: 6.90 ± 0.77; N=4). However, tetramethylrhodamine B isothiocyanate–dextran "LEC labeling" is only feasible in large 4-week-old embryos, but not in small early-stage embryos, precluding us from quantifying Notch-1b expression in early lymphatic development.

Dll4 and Notch-1b were also detected by in situ hybridization in primary ISVs at 30 hpf (Figure 5A-C).[21,22] Because in situ hybridization is technically challenging in embryos beyond 2 dpf, we analyzed Notch expression during LISV-PL migration in *Tp1bglob:eGFPxFli1:DsRed* fish, in which all ECs are red and cells with canonical Notch activity are green (GFP driven by a promoter containing 12 Su[H] binding sequences[13]). Imaging when PL cells turn and switch to radial ventral migration revealed that the DA and aISVs are yellow in the merged image, indicating that canonical Notch signaling was active in arterial vessels but not in LISVs or vISVs (Figure 5E–E'').

Discussion

The key finding of this study is that incomplete silencing or pharmacological inhibition of Notch impaired lymphatic development in zebrafish. Phenotypic analysis indicates that Notch signaling regulates the formation of lymphangiogenic sprouts and their descendent PL cells, which produce the TD (Figure 6A and B). At a later stage, Notch is required for guided migration of LISV-PLs along aISVs (Figure 6C-C''').

Role of Notch in Lymphangiogenic Secondary Sprout Formation

Our results reveal that Notch, in addition to its role in blood vessel morphogenesis and arterial development,[4,9] also regulates lymphatic development. Half of the Notch hypomor-
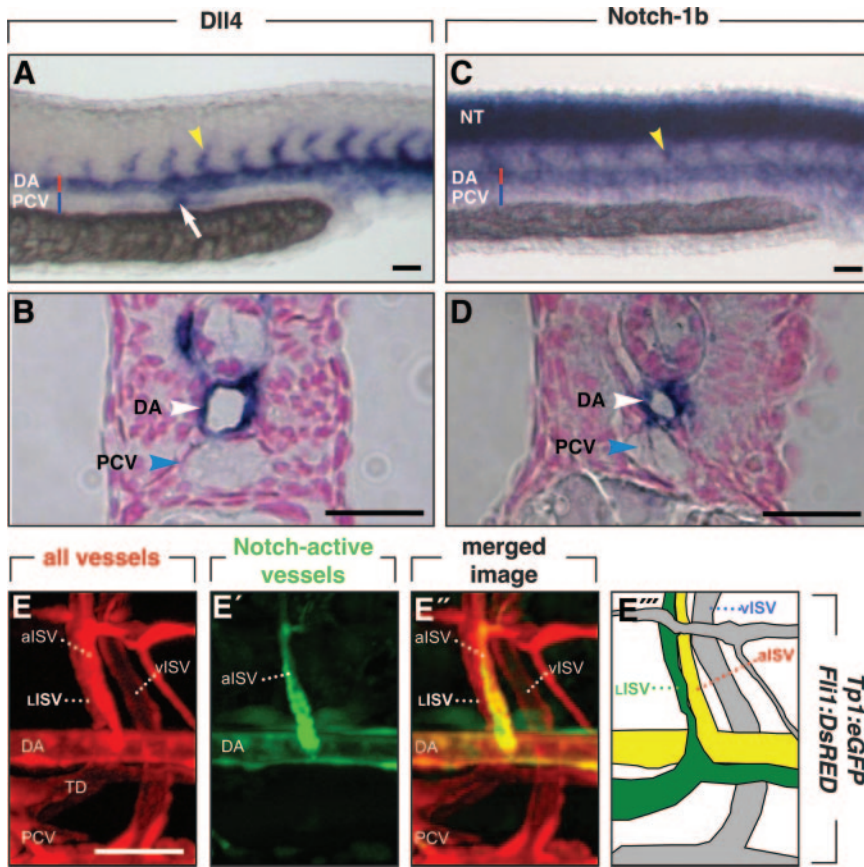
Figure 5. Expression of Dll4/Notch-1b. A through D, Whole-mount stained embryos at 30 hpf, when lymphangiogenic sprouting occurs, stained for Dll4 (A and B) or Notch-1b (C and D). In A and C, primary ISVs are indicated by yellow arrowheads; and in B and D, cross-sections of the respective embryos are shown. In A and B, Dll4 expression was detected in the DA and primary aISVs, pronephric duct (white arrow; A). C and D, Notch-1b is strongly expressed in the neural tube (NT), DA, and primary aISVs. E, Confocal images of *Tp1bglob:eGFPxFli1:DsRed* embryos, in which *Fli1:DsRed* marks blood and lymph vessels in red (E) and *Tp1bglob:eGFP* labels cells with activated canonical Notch activity in green (E'). The merged image shows arterial vessels (DA; aISV) with active Notch in yellow (green-red), whereas the ʟISV are only red (E''). In the schematic representation, the lymphatic structures are indicated in green; Notch-activated vessels, yellow; and other vessels, gray (E'''). Representative images of arterial activation of Notch in a 6-dpf embryo are shown (for technical reasons); however, similar data were obtained at 60 hpf. The bar indicates 50 μm.

phant embryos failed to form a TD without later rescue, indicating lymphatic abortion rather than delay. The earliest identifiable abnormality, the increased fraction of venous ISVs, indicated a defect at the level of the secondary sprouts from the PCV, where fewer lymphangiogenic, but more angiogenic, sprouts developed (Figure 6A and B). Also, most embryos, surviving DAPT treatment at stages when lymphangiogenic sprouting was initiated, did not form a TD, further suggesting an early role for Notch in lymphatic development (data not shown). The hypomorphant pheno-
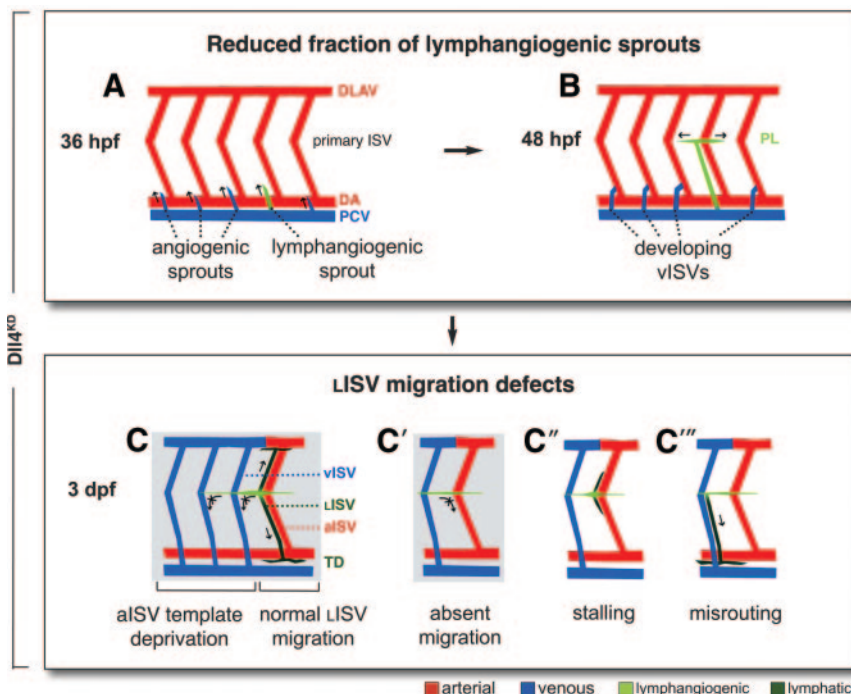
Figure 6. Schematic model of Notch in lymphatic development. Scheme illustrating the different lymphatic defects in Dll4^KD embryos (normal lymphatic development; supplemental Figure I). Permanent lymphatic structures (ʟISV and TD) are dark green; and transient lymphangiogenic structures (lymphangiogenic secondary sprouts and parachordal lymphangioblasts), light green. A and B, Reduced fraction of lymphangiogenic sprouts, resulting in underdevelopment or absence of the PL string, with accompanying overrepresentation of angiogenic secondary sprouts. C through C''', ʟISV migration defects: as a result of vISV overrepresentation, ʟISV-PLs are deprived of their normal aISV guidance template (C) and ʟISV formation is further impaired by additional navigation defects, most frequently because ʟISV-PLs cells bypass their turning point and never initiate ventral radial migration (C') or occasionally make the turn but then stall (C''). More rarely, navigating ʟISV-PLs become misrouted along vISVs (C'''). The most frequent defects are boxed in gray.

typic change correlated with defective formation of the PL and TD and could result from defects in LEC fate acquisition, migration, proliferation, survival, and/or other cellular processes contributing to sprout formation and maintenance.

How Notch signaling regulates lymphatic development remains unresolved. Based on the present study and other recent studies, 3 possible (nonexclusive) models can be considered to explain our findings. A first explanation is that Notch silencing altered blood vessel development and, secondarily, influenced lymphatic development. Previous studies documented that arterial differentiation is impaired by inhibition of multiple Notch signaling pathways (eg, by a dominant-negative Su[H]),[7] but not by selective silencing of Dll4.[21,22] Our imaging and marker expression analyses are consistent with these findings and reveal that initial formation and differentiation of the PCV, DA, and primary ISVs all occurred normally on incomplete silencing of Notch signaling. Thus, at least by generally accepted criteria of arterial and venous identity, these blood vessels developed normally in Dll4[KD] and Notch-1b[KD] embryos. Nevertheless, we do not exclude the possibility that subtle alterations in arterial characteristics of the primary ISVs might have favored supernumerary connections with secondary sprouts, thereby "entrapping" sprouts that would otherwise have remained lymphangiogenic. Also, Notch silencing resulted in a greater fraction of venous than arterial ISVs; because arterial ISVs act as guidance templates for ʟISVs, impaired migration of the latter was indeed attributable to such a change in arterial morphogenesis. However, an outstanding question is whether the aISV changes themselves were, in fact, not caused by defective formation of the lymphangiogenic sprouts in the first instance. Indeed, precisely because lymphangiogenic branches failed to develop in Notch morphants, venous angiogenic sprouts formed instead, which then connected to the primary ISVs and converted them to vISVs.

A second model is that Dll4 and Notch are expressed by the same or adjacent arterial ECs within the DA and that this *cis* signaling induces the release of paracrine lymphangiogenic factors (eg, EphrinB2, VEGF-D,[1,23] or an unknown signal) that indirectly instruct venous ECs of the nearby PCV to induce lymphangiogenic sprout formation in a cell nonautonomous manner. A similar indirect model was proposed to explain segregation of the DA from PCV in zebrafish.[8] Likewise, during ʟISV migration, release of a guidance signal from aISVs in response to Dll4/Notch signaling in arterial cells could assist navigation of ʟISVs to their target projection.

Finally, a third and perhaps the most appealing, but at this stage still speculative, explanation for our data is that arterial Dll4 in the DA signals in *trans* to Notch on ECs in the PCV, which lies in close juxtaposition at the time of lymphangiogenic sprouting. There are arguments in support of and against this model. An argument in favor of a cell autonomous role of Notch in PCV cells is that activation of Notch by Dll4 upregulated several LEC-specific markers in venous ECs in vitro. Expression analysis experiments in vivo yielded inconclusive results. Notch-1b expression was weakly detectable in dispersed dorsal PCV cells, but only at a low level that approached the detection limit of the techniques used. Notch-1b was also measurable by RT-PCR in isolated LECs in older embryos; however, this technique could not be used during early lymphatic development. Therefore, we acknowledge that the Notch-1b expression

results represent a limitation of this study that precludes us from drawing firm conclusions regarding a cell-autonomous role for Notch in lymphangiogenic sprouting.

Another recent study[24] also documented a cell-autonomous role for Notch, whereas a second study[25] did not document this role. In LEC cultures, Notch signaling reprogrammed lymphatic to arterial cell fate, whereas Prox-1 counteracted this force, thereby allowing fine-tuning of the LEC fate in a delicately balanced feedback.[24] These findings are not necessarily contradictory to our findings because they analyzed reprogramming of fully differentiated LECs away from their lymphatic fate; we used venous BECs to study programming toward the LEC fate in vitro. Kang et al[24] note in their discussion that "LEC-fate may not be governed by a two-way turn on-off switch, but rather by a dial switch that allows a *gradient* increase or decrease in the lymphatic cell fate force." Reconciling these and our findings, it seems that Notch levels must be tightly controlled to induce and maintain LEC fate. Low levels of Notch signaling might be required to induce lymphatic fate in venous BECs; once differentiated into LECs, Prox-1 would then secure lymphatic fate by preventing overexpression of Notch because this would promote arterial cell fate.[24] The lower expression of Notch-1 in LECs (as found in the present study and in previous studies[10,24]) than in arterial ECs[8−11] supports this model and could also explain why incomplete Notch silencing sufficed to abrogate lymphatic, but not arterial, development. However, in the absence of more conclusive evidence that Notch silencing abrogates Prox-1 induction in PCV cells in the zebrafish model in vivo, a role for Notch in programming LEC fate remains unproved. Also, Notch may regulate processes other than LEC specification in lymphangiogenic sprouting.

A recent study in mice further adds complexity to this model. Indeed, conditional inactivation of RbpJ, a mediator of canonical Notch signaling, in ECs did not alter the expression of lymphatic markers in venous ECs.[25] Although these data may suggest that Notch signaling is redundant for LEC specification in mammals in vivo, an alternative interpretation is that Notch regulates this process via noncanonical signaling. This might also explain why we could not detect a robust signal in LECs or in their precursors in the *Tp1bglob:eGFPxFli1:DsRed* line. Also, species-specific differences between mammals and zebrafish could account for some of the observations. Overall, whether Notch signaling regulates lymphatic development in a cell-autonomous manner remains to be further elucidated in the future.

Role of Notch in Lymphatic Migration From the PL
Notch signaling also regulated the formation of ʟISVs, which arise from the PL cells. Most frequently, the ʟISV was absent; however, in other rarer cases, migrating ʟISV-PLs stalled or became misrouted (Figure 6C-C‴). Our findings suggest that lymphangiogenic EC migration per se (motility) was normal. Also, we did not detect signs of lymphatic regression or retraction (data not shown). Therefore, it is tempting to speculate that ʟISV defects in Notch-silenced embryos reflect impaired lymphangiogenic cell pathfinding. ʟISV-PLs navigated in close association along aISV templates, raising the question of whether aISVs act as guidance templates for ʟISV-PLs, reminiscent of how follower axons navigate along a pioneer axon's

pathway or how autonomic nerves use arterial tracks to reach their target.[26,27] Therefore, because fewer aISVs are present in Notch morphants as the result of lymphangiogenic sprouting defects, PL cells are deprived of navigation templates and, therefore, cannot form ʟISVs normally (Figure 6C). Other observations that ʟISV-PLs failed to switch from tangential to radial migration or, more rarely, stalled or selected incorrect paths (Figure 6C'-C''') are reminiscent of classic neuronal guidance defects. That arteries may act as navigation templates is evidenced by reports that autonomic nerves stall or become misrouted when these arteries do not produce appropriate guidance cues.[27] Su[H]-dependent Notch activity was detectable in aISVs when PL cells switch from tangential to radial migration alongside aISV, indicating that lymphatic navigation is regulated either cell nonautonomously or via noncanonical Notch signaling. Whether and how Notch regulates the production of turning and guidance cues for ʟISV-PL cells by aISVs or nearby (somitic) cells remain to be determined. Other morphant and mutant zebrafish phenotypes also suggest that ʟISV development requires arterial-lymphatic congruence.[28]

In conclusion, this study revealed a role of Notch in lymphatic development, in part by regulating the initial steps of lymphangiogenic sprouting and PL formation. Moreover, the navigation defects of ʟISV-PL cells along aISVs suggest that Notch also regulates lymph vessel pathfinding along arteries.

Acknowledgments

Sources of Funding

Disclosures

None.

References

1. Tammela T, Alitalo K. Lymphangiogenesis: molecular mechanisms and future promise. *Cell*. 2010;140:460–476.
2. Francois M, Koopman P, Beltrame M. SoxF genes: key players in the development of the cardio-vascular system. *Int J Biochem Cell Biol*. 2010;42:445–448.
3. Gale NW, Thurston G, Hackett SF, Renard R, Wang Q, McClain J, Martin C, Witte C, Witte MH, Jackson D, Suri C, Campochiaro PA, Wiegand SJ, Yancopoulos GD. Angiopoietin-2 is required for postnatal angiogenesis and lymphatic patterning, and only the latter role is rescued by Angiopoietin-1. *Dev Cell*. 2002;3:411–423.
4. De Smet F, Segura I, De Bock K, Hohensinner PJ, Carmeliet P. Mechanisms of vessel branching: filopodia on endothelial tip cells lead the way. *Arterioscler Thromb Vasc Biol*. 2009;29:639–649.
5. Tammela T, Saaristo A, Lohela M, Morisada T, Tornberg J, Norrmen C, Oike Y, Pajusola K, Thurston G, Suda T, Yla-Herttuala S, Alitalo K. Angiopoietin-1 promotes lymphatic sprouting and hyperplasia. *Blood*. 2005;105:4642–4648.
6. Hogan BM, Bos FL, Bussmann J, Witte M, Chi NC, Duckers HJ, Schulte-Merker S. Ccbe1 is required for embryonic lymphangiogenesis and venous sprouting. *Nat Genet*. 2009;41:396–398.
7. Lawson ND, Scheer N, Pham VN, Kim CH, Chitnis AB, Campos-Ortega JA, Weinstein BM. Notch signaling is required for arterial-venous differentiation during embryonic vascular development. *Development*. 2001; 128:3675–3683.
8. Herbert SP, Huisken J, Kim TN, Feldman ME, Houseman BT, Wang RA, Shokat KM, Stainier DY. Arterial-venous segregation by selective cell sprouting: an alternative mode of blood vessel formation. *Science*. 2009;326:294–298.
9. Swift MR, Weinstein BM. Arterial-venous specification during development. *Circ Res*. 2009;104:576–588.
10. Shawber CJ, Kitajewski J. Arterial regulators taken up by lymphatics. *Lymphat Res Biol*. 2008;6:139–143.
11. Emuss V, Lagos D, Pizzey A, Gratrix F, Henderson SR, Boshoff C. KSHV manipulates Notch signaling by DLL4 and JAG1 to alter cell cycle genes in lymphatic endothelia. *PLoS Pathog*. 2009;5:e1000616.
12. Lawson ND, Weinstein BM. In vivo imaging of embryonic vascular development using transgenic zebrafish. *Dev Biol*. 2002;248:307–318.
13. Parsons MJ, Pisharath H, Yusuff S, Moore JC, Siekmann AF, Lawson N, Leach SD. Notch-responsive cells initiate the secondary transition in larval zebrafish pancreas. *Mech Dev*. 2009;126:898–912.
14. Chittenden TW, Claes F, Lanahan AA, Autiero M, Palac RT, Tkachenko EV, Elfenbein A, Ruiz de Almodovar C, Dedkov E, Tomanek R, Li W, Westmore M, Singh JP, Horowitz A, Mulligan-Kehoe MJ, Moodie KL, Zhuang ZW, Carmeliet P, Simons M. Selective regulation of arterial branching morphogenesis by synectin. *Dev Cell*. 2006;10:783–795.
15. Yaniv K, Isogai S, Castranova D, Dye L, Hitomi J, Weinstein BM. Live imaging of lymphatic development in the zebrafish. *Nat Med*. 2006;12:711–716.
16. Kuchler AM, Gjini E, Peterson-Maduro J, Cancilla B, Wolburg H, Schulte-Merker S. Development of the zebrafish lymphatic system requires VEGFC signaling. *Curr Biol*. 2006;16:1244–1248.
17. Ota H, Katsube KI, Ogawa JI, Yanagishita M. Hypoxia/Notch signaling in primary culture of rat lymphatic endothelial cells. *FEBS Lett*. 2007; 581:5220–5226.
18. Geling A, Steiner H, Willem M, Bally-Cuif L, Haass C. A gamma-secretase inhibitor blocks Notch signaling in vivo and causes a severe neurogenic phenotype in zebrafish. *EMBO Rep*. 2002;3:688–694.
19. Hogan BM, Herpers R, Witte M, Helotera H, Alitalo K, Duckers HJ, Schulte-Merker S. Vegfc/Flt4 signalling is suppressed by Dll4 in developing zebrafish intersegmental arteries. *Development*. 2009;136:4001–4009.
20. Lin FJ, Chen X, Qin J, Hong YK, Tsai MJ, Tsai YT. Direct transcriptional regulation of neuropilin-2 by COUP-TFII modulates multiple steps in murine lymphatic vessel development. *J Clin Invest*. 2010;120:1694–1707.
21. Leslie JD, Ariza-McNaughton L, Bermange AL, McAdow R, Johnson SL, Lewis J. Endothelial signalling by the Notch ligand Delta-like 4 restricts angiogenesis. *Development*. 2007;134:839–844.
22. Siekmann AF, Lawson ND. Notch signalling limits angiogenic cell behaviour in developing zebrafish arteries. *Nature*. 2007;445:781–784.
23. O'Neill CF, Urs S, Cinelli C, Lincoln A, Nadeau RJ, Leon R, Toher J, Mouta-Bellum C, Friesel RE, Liaw L. Notch2 signaling induces apoptosis and inhibits human MDA-MB-231 xenograft growth. *Am J Pathol*. 2007; 171:1023–1036.
24. Kang J, Yoo J, Lee S, Tang W, Aguilar B, Ramu S, Choi I, Otu HH, Shin JW, Dotto GP, Koh CJ, Detmar M, Hong YK. An exquisite cross-control mechanism among endothelial cell fate regulators directs the plasticity and heterogeneity of lymphatic endothelial cells. *Blood*. 2010;116:140–150.
25. Srinivasan RS, Geng X, Yang Y, Wang Y, Mukatira S, Studer M, Porto MPR, Lagutin O, Oliver G. The nuclear hormone receptor Coup-TFII is required for the initiation and early maintenance of Prox1 expression in lymphatic endothelial cells. *Genes Dev*. 2010;24:696–707.
26. Bak M, Fraser SE. Axon fasciculation and differences in midline kinetics between pioneer and follower axons within commissural fascicles. *Development*. 2003;130:4999–5008.
27. Makita T, Sucov HM, Gariepy CE, Yanagisawa M, Ginty DD. Endothelins are vascular-derived axonal guidance cues for developing sympathetic neurons. *Nature*. 2008;452:759–763.
28. Bussmann J, Bos LF, Urasaki A, Kawakami K, Duckers HJ, Schulte-Merker S. Arteries provide essential guidance cues for lymphatic endothelial cells in the zebrafish trunk. *Development*. 2010; Epub ahead of print July 7.

SUPPLEMENTAL MATERIAL

ROLE OF DLL4 / NOTCH IN THE FORMATION AND WIRING
OF THE LYMPHATIC NETWORK IN ZEBRAFISH

Geudens et al.

SUPPLEMENTAL METHODS

SCREENING METHODS FOR EVALUATION OF LYMPHATIC DEVELOPMENT AND FUNCTIONALITY

SCORING OF TD AND PL STRING FORMATION IN ZEBRAFISH: Live screening and quantification of thoracic duct (TD) formation was performed on anaesthetized *Fli1:eGFP^{y1}* embryos (a few drops of 4 mg/ml Tricaine (Sigma) stock solution in 5 ml embryo water) at 6 dpf when this vessel was completely developed in control embryos. DAPT treated fish (see below) were screened at 4 dpf, since screening at 6 dpf became impossible because fish became opaque due to loss of trunk circulation and edema and many fish died between 4 and 6 dpf. For screening, images were acquired using Zeiss AxioVision 4.6 software on a Leica DM RBE fluorescence stereomicroscope equipped with a Zeiss AxioCam MrC5 digital camera (Carl Zeiss, Munich, Germany; Leica Microsystems, Wetzlar, Germany). For reasons of standardization and to correct for slight differences in embryo size, the percentage of thoracic duct formation was quantified by scoring its percentile presence in 10 consecutive somite segments in the trunk after the junction of DA and PCV (i.e. somites 5-15, see Supplemental Figure III E). For screening of thoracic duct formation, only embryos with normal overall morphology and normal trunk circulation were included. All data are based on scorings of 33-185 embryos per condition, generated in at least 3 independent experiments. All analyses were performed by investigators blinded for the experimental treatment. Because the penetrance of the lymphatic phenotype was variable (see Supplemental Note II), we also determined the fraction of embryos with severe, intermediate or subtle lymphatic defects for each

treatment dose. Since parachordal lymphangiobast (PL) cells develop initially from lymphangiogenic secondary sprouts in a segmented pattern (Supplemental Figure I),[1] screening of PL string formation in the 10-somite segment of the trunk was performed in a similar manner at 52 hpf. Confocal imaging of *Fli1:eGFP[y1]* embryos was performed using a Zeiss laser scanning microscope LSM510 or Leica SP2, SPE and SP5 confocal microscopes. Embryos were anaesthetized and positioned on a coverslip in a drop of 0.5% low melting point agarose. Fluorescence signal of *Stab1:YFP* images was transformed to a gray-scale image for better contrast.

FUNCTIONAL ASSESSMENT OF THE THORACIC DUCT: For functional studies, anesthetized larvae were subcutaneously injected with 1 nl fluorescent dextran (2.5 mg/ml) into the muscle mass of the posterior trunk by using glass capillaries and a conventional microinjection setup.[2]

IN VIVO "LEC-LABELING" AND FACS SORTING OF LABELED LECS: LEC labeling was performed on anaesthetized (a few drops of 4 mg/ml Tricaine (Sigma) stock solution in 5 ml embryo water) *Fli1:eGFP[y1]* zebrafish larvae of 4 weeks old. Tetramethyl-rhodamine-dextran (TRITC-dextran; molecular weight 2000 kDa) was injected intramuscularly into the tail somites. After 3-4 days the dye had been drained by the lymphatics and was taken up by the LECs through pinocytosis. To obtain single cell suspensions, tails of at least 10 LEC labeled fish were collected, washed with distilled water, chopped, and incubated in 0.25% trypsin at 28°C until almost completely digested. The reaction was stopped by addition of 100μl FCS to inhibit the trypsin and the cell suspension was loaded on top of a Cell strainer tube with blue filter cap (40μm; BD Biosciences) for filtration. After pelleting of the cells (5min, 200g), the cell suspension was washed with 1ml dPBS containing 2% FCS, and viable cells were counted using trypan blue exclusion. After pelleting the cells were resuspended at a concentration of 10^6 cells/ml in FACS buffer (dPBS containing 1% FCS, filtered). Cells were sorted using a FACSAria (Becton Dickinson), taking care to exclude possible doublets or cell clusters. Non-injected GFP$^+$ *Fli1:GFP[y1]* and TRITC-dextran injected GFP$^-$ embryos were used as controls for proper compensation and gate setting. On average 25000 GFP$^+$TRITC$^+$ LECs and 50000 GFP$^+$TRITC$^-$ BECs were sorted directly in lysis buffer (RLT containing 1% β-

mercaptoethanol) and processed for RNA extraction using the RNeasy kit (qiagen).

TIME LAPSE IMAGING: Embryos were mounted in 0.5% low melting point agarose in a culture dish with a cover slip replacing the bottom. Imaging was performed with a Leica SP2 or SP5 confocal microscope using a 10x, 20x or 40x objective with digital zoom. Timelapse analysis was compiled using ImageJ software (http://rsb.info.nih.gov/ij/). Time points were recorded every 10 minutes for the stated time period. A heated stage maintained the embryos at approximately 28.3 °C.

WHOLE-MOUNT IN SITU HYBRIDIZATION: Antisense probes specific for zebrafish *EphrinB2a,*[3] *Vegfr3,*[4] *Notch-1b, Notch-6, Dll4, Tie2, Dab2,*[1, 5] *Tbx20,*[6] *Cmlc2* or *MyoD* were used for whole-mount *in situ* hybridization of 28-48hpf embryos as described.[7] Stained embryos were paraffin- or plastic-embedded, sectioned and counterstained with nuclear fast red. In all figure panels the head of the embryo faces left and dorsal is up, unless stated otherwise.

QUANTITATIVE RT-PCR EXPRESSION ANALYSIS: RNA from FACS sorted LECs was reverse transcribed using the SuperScriptIII kit from Ambion. RNA from whole embryos was obtained by lysing in Trizol reagent and extraction using the RNeasy MiniElute Cleanup kit (Qiagen) and cDNA was prepared using the Quantitect Reverse Transcription kit (Qiagen). cDNA was subjected to qRT-PCR using zebrafish gene-specific primers/probe sets (Table S2).

CELL CULTURE EXPERIMENTS

HUVEC cells (Lonza, Invitrogen, Merelbeke, Belgium) and HUVEC/COS co-cultures were grown in EGM2-MV medium (Lonza, Invitrogen) at 37°C. COS cells were grown in standard DMEM medium (Lonza, Invitrogen) supplemented with 10% FBS, 2 mM glutamin, 100 U/ml penicillin, and 0.1 mg/ml streptomycin (Lonza).

COCULTURE ASSAY: COS cells stably expressing full length human Dll4 (COS^{Dll4}) or expressing GFP (COS^{CTR}) were prepared using the retroviral constructs LZRSpBMN-DLL4 and LZRSpBMN-WT, respectively.[8] HUVECs were co-seeded with COS^{Dll4} or COS^{CTR} cells in 6-wells at a density of 200,000 cells each, grown for 24 hours and harvested for RNA analysis by quantitative RT-PCR using human

gene-specific primers (Table S2). *PROLIFERATION ASSAY:* Primary LEC (HMVEC-DLy or HMVEC-LLy; Lonza, Invitrogen) were starved overnight in EGM2 medium (Lonza, Invitrogen) containing 0.1% serum and no growth factors (starvation medium). The starved cells were seeded at 2,000 cells per well in 96-well microtiter plates, after which proliferation was induced with fully supplemented EGM2-MV medium with or without increasing concentrations of DAPT (20-60 μM). Proliferation was measured as the number of viable cells after further culturing for 48 hours, expressed in % of DMSO control. Viable cells were quantified using the Rapid Cell Proliferation assay (Calbiochem, San Diego, CA).

SCRATCH WOUND MIGRATION ASSAY: Confluent monolayers of LECs growing in 0.1% gelatin-coated wells of a 24-well plate were starved overnight, pretreated in starvation medium containing 30 μM DAPT or 0.3% DMSO (control), scratch wounded and photographed (T0). The cells were further incubated for 24 hrs and photographed again (T24). Migration distance (gap width at T0 minus gap width at T24; 10 measurements per wound at regular intervals along the wound) was determined by image analysis using KS300 morphometry software, and is expressed relative to the control (DMSO).

TRANSWELL MIGRATION ASSAY IN CONDITIONS OF NOTCH INHIBITION: LECs were pretreated with DAPT (60 μM) or vehicle (DMSO) in starvation medium overnight, seeded at 30,000 cells per transwell on 0.1% gelatin-coated transwells in starvation medium with DAPT or DMSO, and cultured for 2 hours until adherence. Migration was induced by transferring the transwell insets into wells (bottom well) containing fully supplemented EGM2-MV medium with 100 ng recombinant human VEGF-C (Reliatech, TecoMedical NL, Nijkerk, the Netherlands), and DAPT or DMSO. Background migration was determined by including transwells with starvation medium in both the top and bottom well (baseline). After culturing for 16 hours, the non-migrated cells on the top side of the transwell filters were wiped off using PBS-soaked cotton swabs, and the transwells were fixed with 1% p-formaldehyde. The transwell filters were cut out and mounted upside-down on micrsocope slides with DAPI containing mounting medium. The filters were photographed under DAPI fluorescence at 20x magnification, and the nuclei were counted as a measure of

migrated cells. Five transwells were prepared per condition and five optical fields were counted and averaged per transwell filter.

TRANSWELL MIGRATION ASSAY IN CONDITIONS OF NOTCH ACTIVATION: LECs were starved overnight and seeded at 30,000 cells per transwell on transwell filters coated with BSA or with the extracellular domain of Dll4 (Dll4-ECD; R&D Systems Europe Ltd., Abingdon, UK) to activate the Notch pathway as described.[9] Further manipulation was as described above, using starvation medium in all top wells and fully supplemented medium containing VEGF-C in all bottom wells except for the baseline conditions. The filters were photographed under DAPI fluorescence at 10x magnification, Five transwells were prepared per condition and 1 central optical field was counted per transwell filter.

SUPPLEMENTAL NOTES

SUPPLEMENTAL NOTE I: LYMPHATIC DEVELOPMENT IN ZEBRAFISH EMBRYOS

In zebrafish embryos, the thoracic duct (TD) develops between the dorsal aorta (DA) and posterior cardinal vein (PCV); it is considered to be the first perfused lymphatic, as it drains interstitial dyes and has structural characteristics closely resembling mammalian lymphatics.[2, 10, 11] For reasons of clarity, formation of this early lymphatic network is schematically illustrated in Supplemental Figure I. Around 30 hpf, half of the secondary sprouts from the PCV, on average one per two unilateral somite segments, migrate radially in the ventral-dorsal direction to the horizontal myoseptum; these sprouts exist transiently (Supplemental Figure I A,A',B,B').[1, 12] At the horizontal myoseptum, cells of these sprouts then migrate tangentially in the anterior-posterior direction to form a string of parachordal lymphangioblasts (PL), which act as progenitors of future LECs in the TD (36 to 60 hpf); the PL string also exists only transiently. Since the secondary sprouts from the PCV, which give rise to the PL, participate in the process that leads to the formation of the TD, they have been termed "lymphangiogenic secondary sprouts". Indeed, the lymphangiogenic sprouts and PL cells give rise only to lymphatics but not to blood vessels, are not labeled in the arterial/venous *kdr-l:mCherryRed* marker line,[1] and fail to form upon silencing of genes that regulate lymphangiogenesis in mice and humans, e.g., *Ccbe1,*[1, 13] *Vegf-c,*[1] *Vegfr-3*[14] and *Synectin* (unpublished). The other secondary sprouts connect to the primary intersomitic vessels (ISVs), which thereby become intersomitic veins (vISV), and have therefore been termed "angiogenic secondary sprouts" (Supplemental Figure I A,B).[1, 12]

From 60 hpf onwards, the PL cells switch to radial migration again, and navigate both ventrally and dorsally alongside arterial intersomitic vessels (aISVs), whereby they form structures, that later persist as lymphatic intersomitic vessels (ʟISVs) (Supplemental Figure I C,D).[1] These radially migrating cells are termed ʟISV-PLs to distinguish them from the cells in the PL string. Once ventrally migrating ʟISV-PLs

reach their final location in-between the DA and PCV, they switch again to tangential migration, grow towards each other and fuse to establish the TD (3 to 6 dpf) (Supplemental Figure I D,D').[1, 2, 11, 12] While lymphangiogenic secondary sprouts migrate at a distance from and independently of aISVs, LISVs always navigated alongside aISVs, almost "creeping" over them in their initial dorsal and ventral trajectory, but never track alongside vISVs (Supplemental Figure I A',B',D'). This close association of LISVs with aISVs raised the question whether aISVs act as guidance templates for navigating LISVs-PLs.

SUPPLEMENTAL NOTE II: SILENCING STRATEGIES TO STUDY THE ROLE OF NOTCH IN LYMPH VESSEL FORMATION

SILENCING STRATEGIES: To explore a role for Notch signaling in lymphatic development, we made use of morpholino antisense oligonucleotides to silence every known zebrafish orthologue of the Notch ligands (DeltaA-D, Dll4, Jagged-1a/b, Jagged-2) and receptors (Notch-1a/b, -5, -6) as well as of the Notch activating presenilins (PS-1 and PS-2). For reasons of consistency, we used the zebrafish nomenclature: zebrafish Notch-5 and -6 are mammalian homologues of Notch-3 and -2, respectively, while zebrafish Notch-1a and -1b are duplicated mammalian orthologues of Notch-1.[15] Alternatively, Notch receptor activation was inhibited by exposing dechorionated 24-hpf embryos to *N*-[N-(3,5-difluorophenacetyl)-L-alanyl]-S-phenylglycine t-butyl ester (DAPT), a well known γ-secretase inhibitor (γ-secretase inhibitor IX; Calbiochem), that has been previously used to block Notch signaling in zebrafish embryos.[16]

SPECIFICITY OF THE PHENOTYPES: As Notch-family members have been implicated in angiogenesis,[17-19] we used submaximal doses of all morpholinos or of compound inhibitor to minimize secondary effects of vascular malformations on lymphatic development (referred to as "incomplete silencing" and "Notch hypomorphants"; Supplemental Figure II A-H and not shown). Furthermore, the compound inhibitor DAPT was added at later developmental stages, to avoid defects in early vascular development. We experimentally determined that treatment initiation at 43 hpf

induced lymphatic defects without inducing major vascular and developmental malformations. Treatment at earlier stages induced blood flow arrest, hemorrhages and edema in the majority of treated embryos. Only morphant embryos with a normal size, trunk circulation and blood flow, and without developmental delay, tissue malformations, general edema or toxic defects were included (Supplemental Figure III A-D; not shown). The lymphatic defects upon knockdown or compound treatment indeed were specific, as no overt changes in the formation and differentiation of the DA and PCV were noticeable (Supplemental Figure IV). Consistent with previous reports,[14, 20] some hyperbranching of the primary ISVs was detected in Dll4[KD] hypomorphant embryos, but to a variable degree and in only 20% of Dll4[KD] embryos (red arrowheads in Figure 1B; Supplemental Movie II). Also, no abnormalities in heart or somite development were observed (Supplemental Figure II I-L).

PHENOTYPE PENETRANCE: We speculate that the variably penetrant lymphatic phenotypes and spectrum of defects in the Notch hypomorphants is due to a combination of reasons, including the use of a submaximal dose of morpholino (incomplete silencing), technical limitations of injecting an identical dose of morpholino, genetic differences of the morphant embryos analyzed (outbred background; 10-fold variable RNA expression levels were observed for Dll4 between individual 4-dpf old embryos (copies Dll4/10^5 copies β-actin, median (range): 23.4 (6 – 58); *N*=24), uneven dispersion of morpholinos upon daughter cell division, and variable timing of venous/lymphatic secondary sprout formation along the PCV (occurring within a time window of 30 to 50 hpf [1]). As a result, achieving the necessary degree of silencing below the critical biological threshold at the distinct sprouting locations along the PCV becomes stochastic in such experimental conditions.

Phenotypic defects were dose-dependent, but for reasons of brevity, only the highest dose is shown. A standard control morpholino was used routinely and results were confirmed by using a second independent target-specific morpholino for silencing of Dll4, Notch-1b and PS-1.

SUPPLEMENTAL NOTE III: ACRONYMS FOR VASCULAR AND LYMPHATIC STRUCTURES IN THE ZEBRAFISH MODEL

aISV: arterial intersomitic vessel

BEC: blood endothelial cell

DA: dorsal aorta

DLAV: dorsal longitudinal anastomosing vessel

DLLV: dorsal longitudinal lymphatic vessel

ISV: intersomitic vessel

LEC: lymphatic endothelial cell

ʟISV: lymphatic intersomitic vessel

ʟISV-PL: parachordal lymphangioblasts that form the ʟISV

PAV: parachordal vessel

PCV: posterior cardinal vein

PL: parochordal lymphangioblast

TD: thoracic duct

vISV: venous intersomitic vessel

SUPPLEMENTAL FIGURES and MOVIES

SUPPLEMENTAL FIGURE I: MODEL OF LYMPHATIC DEVELOPMENT IN ZEBRAFISH EMBRYOS

In all panels, a schematic figure is shown on the left, and for panel A,B,D a high-magnification image of the blood and lymphatic vasculature at different stages of development in *Fli1:eGFP^{y1}* zebrafish on the right. For clarity, the confocal images are flanked by redrawings of the vessel contours. DA, dorsal aorta; DLAV, dorsal longitudinal anastomosing vessel; DLLV, dorsal longitudinal lymph vessel; ISV, intersomitic vessel; aISV, arterial ISV; LISV, lymphatic ISV; vISV, venous ISV; PCV, posterial cardinal vein; PL, parachordal lymphangioblast string; TD, thoracic duct. Permanent lymphatic structures (LISV, TD) are labeled dark green; transient lymphangiogenic structures (lymphangiogenic secondary sprouts; PL cells) are labeled light green. **A,A',** From around 30 hpf onwards, secondary sprouts arise from the PCV. About half of them will give rise to lymphatic structures and are therefore named lymphangiogenic secondary sprout (Ly sec. sprout; yellow arrows in A'). The other half of the secondary sprouts remain venous in nature (angiogenic secondary sprouts) (blue in A). **B,B',** By 48 hpf, the lymphangiogenic sprouts (yellow arrows in B') radially migrate dorsally to the level of the horizontal myoseptum, where they migrate tangentially to give rise to a transiently existing string of PL cells. The angiogenic sprouts connect to the aISV (red), which thereby will acquire a venous identity. **C,** Around 60 hpf, PL cells turn and switch from tangential to radial migration closely along aISVs, thereby forming lymphatic intersomitic vessels (LISVs); note the close association of LISVs with aISVs. LISVs that ascend form the dorsal longitudinal lymph vessel (DLLV), while those that descend form the TD. ISVs that connected to the angiogenic secondary sprouts progressively loose their arterial identity and acquire a venous fate. **D,D',** From 3 days onwards, the first TD fragments appear at distinct locations along the trunk and, via tangential migration, extend rostrally and caudally to merge into a complete TD. The LISV and TD are indicated by white arrows and arrowhead, respectively, in D'.

SUPPLEMENTAL FIGURE II: DEVELOPMENT OF EMBRYOS UPON INCOMPLETE INHIBITION OF DLL4

Complete silencing of Dll4/Notch signaling causes pronounced angiogenic defects.[17, 18, 21, 22] We therefore performed a detailed analysis, using high-resolution imaging, of the vasculature of control (A,C,E,G) and Dll4^{KD} hypomorphant *Fli1:eGFP^{y1}* embryos (10 ng Dll4^{SPL}; B,D,F,H). Scale bars: 100 μm. DA, dorsal aorta; PAV, parachordal vessel; PCV, posterior cardinal vein; TD, thoracic duct. **A,B,** The early vasculogenic stages proceeded normally in morphant embryos, resulting in the formation of properly sized and shaped axial vessels at timely developmental stages. Knockdown of Dll4 did not affect the timing or pathfinding of primary ISVs, or the subsequent formation of the DLAV (arrows) in embryos at 30 hpf. The DA is indicated by a red vertical bar, while the PCV is denoted by a blue vertical bar. **C,D,** Close-up images of the head vasculature at 30 hpf, showing similar appearance in control and Dll4^{KD} embryos. The arrow denotes the mid-cerebral vein. **E,F**, The subintestinal vessels (arrows) in 3-dpf Dll4^{KD} embryos displayed a largely comparable network morphogenesis with only minimal signs of hyperbranching. **G,H,** Image of a 12-dpf embryo, revealing that knockdown of Dll4 did not prevent the formation of the PAV, which develops only after the TD is established. Note the absence of the TD in the morphant embryo (asterisks in panel H), indicating that the TD defect persisted and was not rescued over time. The yellow arrowheads in G denote the course of the TD in the control embryo. The red arrowheads in H denote mild hyperbranching of the ISVs in the Dll4^{KD} embryo. **I-L,** Whole-mount *in situ* stainings for *Cmlc2* (I,J; 30 hpf) and *MyoD* (K,L; 48 hpf), showing that size and positioning of the heart (arrow) and somite development are normal in Dll4^{KD} embryos. Overall, at the morpholino concentrations used in our analyses, no overt angiogenic malformations were detected in Dll4^{KD} embryos prior to or during lymphangiogenesis. Further, imaging of the *Flt1:YFP* reporter line, in which only arterial ECs are labeled, confirmed that primary aISVs expressed the YFP transgene in Dll4^{KD} embryos, indicating that their initial arterial specification occurred normally (see Supplemental Movie II).

SUPPLEMENTAL FIGURE III: GENERAL MORPHOLOGY AND ANALYSIS OF TD FORMATION

A-D, Bright field images of 6-dpf control (A), Dll4^{KD} (10 ng Dll4^{SPL}; B), Notch-1b^{KD} (15 ng Notch-1b^{SPL}; C) and Notch-6^{KD} (15 ng Notch-6^{SPL}; D) embryos, showing normal overall morphological development. Only morphant embryos with a normal trunk circulation and body size, without developmental delay, tissue malformations, general edema or toxic defects were included in TD screening assays. **E,** TD quantification. DA, dorsal aorta; DLAV, dorsal longitudinal anastomosing vessels; ISV, intersomitic vessel; PCV, posterial cardinal vein; PL, parachordal lymphangioblast string; TD, thoracic duct. TD formation was quantified by measuring the length over which it formed in 10 consecutive somite segments (i.e. somites 5-15; demarcated by the green rectangle). Confocal images of control and morphant *Fli:eGFP^{y1}* embryos are depicted in the insets. Inset a: in the control embryo, a continuous TD formed over all 10 somite segments (100% TD formation; green arrowheads). Inset b: severely morphant embryo, in which the TD formed over only 10% (green arrowhead). Inset a' and b': schematic redrawing of the DA, TD and PCV in the embryo shown in inset a and b, respectively, with the TD or TD segment marked in green. Scale bars: 200 μm in A-D, 100 μm in E and insets of E.

SUPPLEMENTAL FIGURE IV: NORMAL ARTERIAL-VENOUS DIFFERENTIATION AFTER INHIBITION OF NOTCH.

A-R, Arterial-venous differentiation of the large axial vessels was evaluated upon incomplete silencing of the components of the Dll4/Notch signaling pathway that were shown in this study to affect lymphatic development. Therefore, whole-mount embryos were *in situ* stained for arterial (*EphrinB2a; Tbx20* [6, 23]) and venous (*Vegfr3; Dab2* [5, 24]) markers in control embryos (A-D) and in Dll4^{KD} (10 ng Dll4^{SPL}; E-H), Notch-1b^{KD} (15 ng Notch-1b^{SPL}; I-L), Notch-6 (15 ng Notch-6^{SPL}; M,N), PS-1 (15 ng PS-1^{ATG1}; O,P) or DAPT-treated (25 μM; Q,R) hypomorphic embryos. Staining was performed at 28 hpf (few hours prior to secondary sprout formation) for *EphrinB2a, Vegfr3 and Tbx20,* and at 48 hpf for *Dab2*, when arterial and venous differentiation of the DA and PCV were completed. Overall, expression of arterial markers in the DA and of venous markers in the PCV was comparable in control and morphant

embryos. Also, note that there is no ectopic expression of these markers. The DA is indicated by a red vertical bar, while the PCV is denoted by a blue vertical bar. DA, dorsal aorta; PCV, posterior cardinal vein. Scale bar, representative for all panels: 100 μm.

SUPPLEMENTAL FIGURE V: INHIBITION OF NOTCH DOES NOT AFFECT *IN VITRO* PROLIFERATION AND MIGRATION.

A, Primary LECs of dermal (HMVEC-DLy) and lung (HMVEC-LLy) origin were starved overnight, after which proliferation was induced with full growth medium with or without increasing concentrations of DAPT (30-60 μM). Proliferation was measured as the number of viable cells after further culturing for 48 hours, expressed in % of control. **B**, Migration of LECs, analyzed using a scratch wound healing assay, was not inhibited by DAPT (30 μM). **C**, Transwell migration of LECs in response to culture medium containing 10% FBS and 100 ng/ml VEGF-C in the lower compartment ("stimulated") was not affected by DAPT (60 μM). **D**, Transwell migration of LECs in response to culture medium containing 10% FBS and 100 ng/ml VEGF-C in the lower compartment was comparable, when cells were seeded on filters coated with BSA (control) or the extracellular domain of Dll4 (Dll4-ECD), previously shown to activate Notch signaling.[9] Error bars represent SEM; *N*=5-11.

SUPPLEMENTAL FIGURE VI: EXPRESSION OF NOTCH-1B.

Sagital section of an embryo at 30 hpf, when lymphangiogenic sprouting occurs, whole-mount stained for Notch-1b. DA, dorsal aorta; ISV, intersomitic vessel; PCV, posterior cardinal vein. Scale bar: 50 μm. Notch-1b is expressed in the DA and ISVs. A weak signal can be observed in the dorsal part of the PCV.

SUPPLEMENTAL MOVIE I: NORMAL FORMATION OF ARTERIAL AND VENOUS ISVS IN CONTROL EMBRYOS.

Confocal time-lapse video-imaging analysis of a control *Flt1:YFPxkdr-I:mCherryRed*

reporter embryo from 32 to 72 hpf (representative movie of >100 embryos analyzed), in which venous cells are red (CherryRed[+]) and arterial cells yellow (YFP[+]CherryRed[+]). Imaging revealed normal progressive ventral-to-dorsal loss of the arterial YFP colour in approximately half of the ISVs, once connected by angiogenic secondary sprouts of the PCV. For instance, the second and third primary ISV (numbering according to the location at the start of the movie) retain their connection with the DA as well as their yellow arterial colour, and are thus arterial. In contrast, the fourth and fifth ISV loose their connection with the DA as well as their yellow arterial colour, progressively become red after establishing a connection with the PCV, and thus become venous ISVs.

Note: This *Flt1:YFPxkdr-l:mCherryRed* reporter does not label lymph vessels. However, since lymphangiogenic secondary sprouts emanate from the PCV (CherryRed[+]) and the CherryRed protein is only degraded after some time, the presence of these lymphangiogenic secondary sprouts and of the PL cells is also transiently visible. For instance, around 40 hpf, red lymphangiogenic secondary sprouts can be seen adjacent to the second and third ISV. These secondary sprouts do, however, not connect to the primary ISVs, but migrate dorsally to the horizontal myoseptum, where they then migrate tangentially and form the PL string. The lymphangiogenic nature of the PL string is illustrated by the gradual loss of its residual mCherryRed colour beyond 52 hpf; this is not due to regression of the PL cells, since this string disappears only around 4 dpf, i.e. after giving rise to the ʟISVs (not visible in this reporter line) that descend ventrally to the level between the DA and PCV to form the TD. DA, dorsal aorta; PCV, posterior cardinal vein; PL, parachordal lymphangioblast string; TD, thoracic duct.

SUPPLEMENTAL MOVIE II: ARTERIAL-TO-VENOUS SHIFT OF ISVS IN DLL4[KD] EMBRYOS

Confocal time-lapse video-imaging analysis of a Dll4[KD] *Flt1:YFPxkdr-l:mCherryRed* embryo from 32-72 hpf (representative movie of >100 embryos analyzed), in which venous cells are red (CherryRed[+]) and arterial cells yellow (YFP[+]CherryRed[+]). Imaging revealed progressive ventral-to-dorsal loss of the arterial YFP colour in all primary ISVs, when they became connected by an angiogenic secondary sprout and

therefore adopted a venous fate. In this embryo, there was a shift of lymphangiogenic to angiogenic secondary sprouting in all somites imaged.

SUPPLEMENTAL TABLE I: MORPHOLINO OLIGONUCLEOTIDE SEQUENCES

MO	MO sequence	Target	Ref
DeltaA[ATG]	5'-CGCCGACTGATTCATTGGTGGAGAC-3'	Start site	
DeltaB[ATG]	5'- CGCCATCTCGCTCACTTTATCCTAA-3'	Start site	
DeltaC[ATG]	5'- GCACGTTAATAAAACACGAGCCATC-3'	Start site	
DeltaD[ATG]	5'- AACAGCTATCATTAGTCGTCCCATG-3'	Start site	
Dll4[ATG]	5'-GAGAAAGGTGAGCCAAGCTGCCATG-3'	Start site	
Dll4[SPL]	5'-TAGGGTTTAGTCTTACCTTGGTCAC-3' 5'-TGATCTCTGATTGCTTACGTTCTTC -3'	Exon6/intron6 Exon4/intron4	20
Jag1a[ATG]	5'-GTCTGTCTGTGTGTCTGTCGCTGTG-3'	5' UTR	
Jag1b[ATG]	5'-CTGAACTCCGTCGCAGAATCATGCC-3'	Start site	
Jag2[ATG]	5'-TCCTGATACAATTCCACATGCCGCC-3'	Start site	
Notch-1a[ATG]	5'-TTCACCAAGAAACGGTTCATAACTC-3'	Start site	25, 26
Notch-1b[ATG]	5'-ATGCATTCCTTCTTATGGATAGTCC-3'	Start site	
Notch-1b[SPL]	5'-AATCTCAAACTGACCTCAAACCGAC-3'	intron28/exon29	20, 27
Notch-5[ATG]	5'-ATATCCAAAGGCTGTAATTCCCCAT-3'	Start site	20, 28
Notch-6[SPL]	5'-AGGTGAACACTTACTTCATGCCAAA-3'	exon7/intron7	20, 28
PS-1[ATG1]	5'-CCGGGATCATAGAAACAGCGGGAAC-3'	5' UTR	
PS-1[ATG2]	5'-CATTCTGCACTAAATCAGCCATCGG-3'	Start site	
PS-2[ATG]	5'-CTCTTCACTGTCTGAGGTATTCATG-3'	Start site	29
control MO	5'-CCTCTTACCTCAGTTACAATTTATA-3'	Standard control MO (Gene Tools)	

For the previously unpublished morpholinos, silencing efficiencies of morpholinos directed against the ATG region were confirmed using a luciferase reporter assay, as previously described [30] (not shown).

SUPPLEMENTAL TABLE S2: qRT-PCR PRIMER AND PROBE SEQUENCES

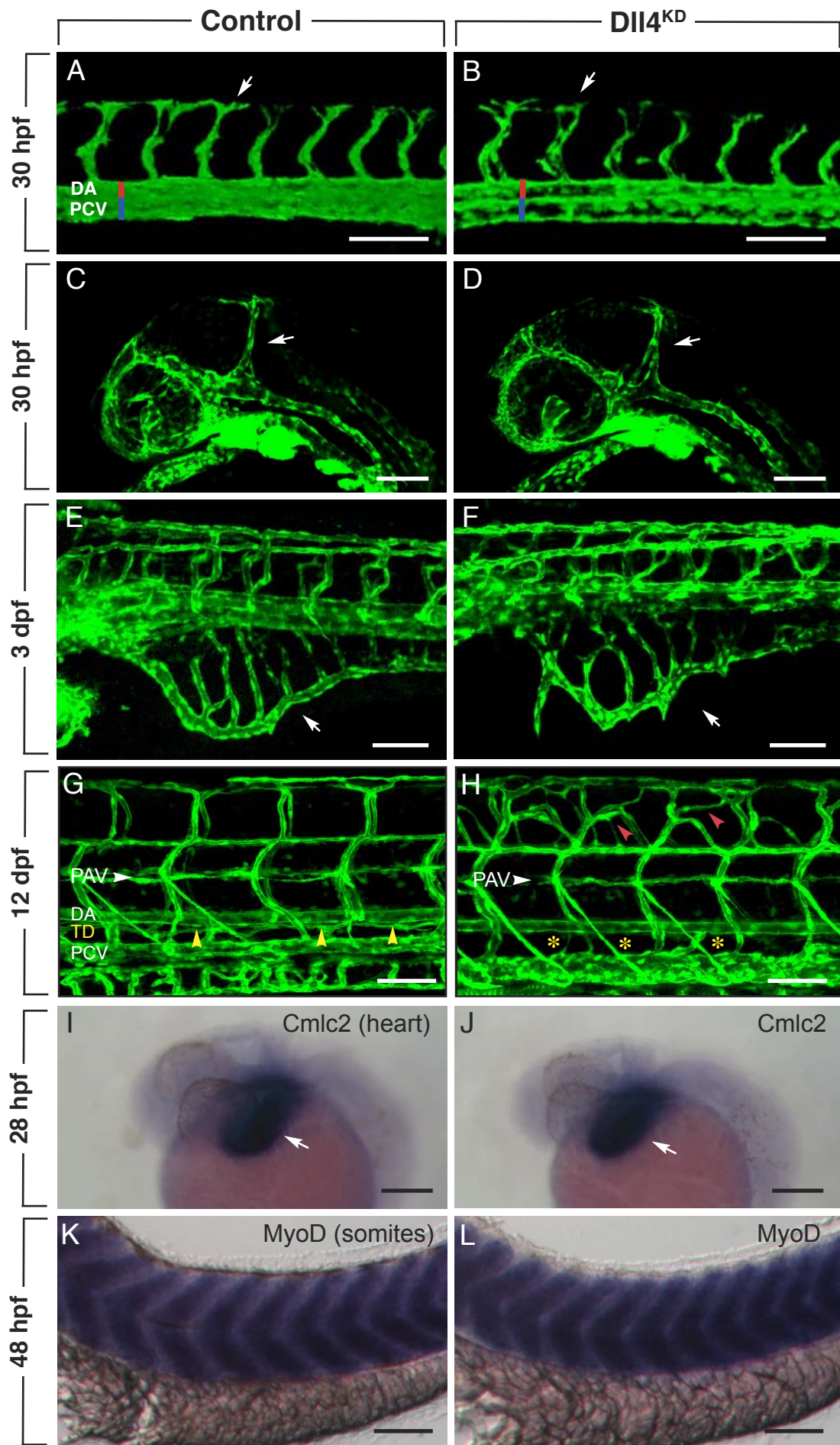| Zebrafish genes		
NOTCH1B	For Rev Probe	5'-AAC AAC CAA GAT CTT TCC CAT ATA CA-3' 5'-GCT CTA GCC ATT CGC ATT GAC-3' 5'-FAM-TTT GAT CCA TTG CCT CCA CGT CTC ACT-TAMRA-3'
DLL4	For Rev Probe	5'-CTT CAC CGG ACC CCT CTG T-3' 5'-TGG AAG CGG TCT TGA GTT TCT C-3' 5'-FAM-ATA CTA CGC CGT CAC AGC GCC CG-TAMRA-3'
β-ACTIN	For Rev Probe	5'-TGG TAT GGG ACA GAA AGA CAG CT-3' 5'-TTG GGT ACT CAG GGT CAG GA-3' 5'-FAM-TCT TGC TCT GAG CCT CAT CAC CAA CG-TAMRA-3'
Human genes		
HES1		Hs00232622_m1 (Premade Taqman Gene expression assays, Applied Biosystems)
HEY1		Hs00232618_m1 (Premade Taqman Gene expression assays, Applied Biosystems)
HEY2		Hs00232622_m1 (Premade Taqman Gene expression assays, Applied Biosystems)
NRARP		Hs01104102_s1 (Premade Taqman Gene expression assays, Applied Biosystems)
VEGFR3	For Rev Probe	5'-TTC CTG GCT TCC CGA AAG T-3' 5'-AGG CCA AGT CAC AGA TCT TCA C-3' 5'-FAM-ACC TGG CTG CTC GGA ACA TTC TGC-TAMRA-3'
PROX-1	For Rev Probe	5'-GTG CTT TGG CGA CGT CAT C-3' 5'-TCA GTG GAA CTG GCC ATC TG-3' 5'-FAM-TTC CGA ACC CCC TGG ACA CCT TTG-TAMRA-3'
LYVE-1	For Rev Probe	5'-CAA AGA TCC CAT ATT CAA CAC TCA A-3' 5'-GGG ATG CCA CCG AGT AGG TA-3' 5'-FAM-CTG CAA CAC AAA CAA CAG AAT TTA TTG TCA GTG ACA-TAMRA-3'
EPHRINB2		Hs00970627_m1 (Premade Taqman Gene expression assays, Applied Biosystems)
SOX18	For Rev	5'-AGA ACC CGG ACC TGC ACA-3' (Sybr Green qRT-PCR) 5'-CAG CTC CTT CCA CGC TTT G-3'
COUP-TFII		Hs00819630_m1 (Premade Taqman Gene expression assays, Applied Biosystems)
NEUROPILIN2		Hs00187290_m1 (Premade Taqman Gene expression assays, Applied Biosystems)
CD31	For Rev	5'-TCT GCA CTG CAG GTA TTG ACA A-3' (Sybr Green qRT-PCR) 5'-CTG ATC GAT TCG CAA CGG A-3'
VE-CADHERIN		Hs00174344_m1 (Premade Taqman Gene expression assays, Applied Biosystems)
ENDOGLIN		Hs00164438_m1 (Premade Taqman Gene expression assays, Applied Biosystems)
β-ACTIN		Hs99999903_m1 (Premade Taqman Gene expression assays, Applied Biosystems)
β-ACTIN	For Rev	5'-TGG CAC CAC ACC TTC TAC AAT G-3' (Sybr Green qRT-PCR) 5'-TAG CAA CGT ACA TGG CTG GG-3'

REFERENCES

1. Hogan BM, Bos FL, Bussmann J, Witte M, Chi NC, Duckers HJ, Schulte-Merker S. Ccbe1 is required for embryonic lymphangiogenesis and venous sprouting. *Nat Genet.* 2009;41:396-398.
2. Kuchler AM, Gjini E, Peterson-Maduro J, Cancilla B, Wolburg H, Schulte-Merker S. Development of the zebrafish lymphatic system requires VEGFC signaling. *Curr Biol.* 2006;16:1244-1248.
3. Chan J, Mably JD, Serluca FC, Chen JN, Goldstein NB, Thomas MC, Cleary JA, Brennan C, Fishman MC, Roberts TM. Morphogenesis of prechordal plate and notochord requires intact Eph/ephrin B signaling. *Dev Biol.* 2001;234:470-482.
4. Thompson MA, Ransom DG, Pratt SJ, MacLennan H, Kieran MW, Detrich HW, 3rd, Vail B, Huber TL, Paw B, Brownlie AJ, Oates AC, Fritz A, Gates MA, Amores A, Bahary N, Talbot WS, Her H, Beier DR, Postlethwait JH, Zon LI. The cloche and spadetail genes differentially affect hematopoiesis and vasculogenesis. *Dev Biol.* 1998;197:248-269.
5. Herpers R, van de Kamp E, Duckers HJ, Schulte-Merker S. Redundant roles for sox7 and sox18 in arteriovenous specification in zebrafish. *Circ Res.* 2008;102:12-15.
6. Szeto DP, Griffin KJ, Kimelman D. HrT is required for cardiovascular development in zebrafish. *Development.* 2002;129:5093-5101.
7. Chittenden TW, Claes F, Lanahan AA, Autiero M, Palac RT, Tkachenko EV, Elfenbein A, Ruiz de Almodovar C, Dedkov E, Tomanek R, Li W, Westmore M, Singh JP, Horowitz A, Mulligan-Kehoe MJ, Moodie KL, Zhuang ZW, Carmeliet P, Simons M. Selective regulation of arterial branching morphogenesis by synectin. *Dev Cell.* 2006;10:783-795.
8. Williams CK, Li JL, Murga M, Harris AL, Tosato G. Up-regulation of the Notch ligand Delta-like 4 inhibits VEGF-induced endothelial cell function. *Blood.* 2006;107:931-939.
9. Harrington LS, Sainson RC, Williams CK, Taylor JM, Shi W, Li JL, Harris AL. Regulation of multiple angiogenic pathways by Dll4 and Notch in human umbilical vein endothelial cells. *Microvasc Res.* 2008;75:144-154.
10. Jensen LD, Cao R, Hedlund EM, Soll I, Lundberg JO, Hauptmann G, Steffensen JF, Cao Y. Nitric oxide permits hypoxia-induced lymphatic perfusion by controlling arterial-lymphatic conduits in zebrafish and glass catfish. *Proc Natl Acad Sci U S A.* 2009.
11. Yaniv K, Isogai S, Castranova D, Dye L, Hitomi J, Weinstein BM. Live imaging of lymphatic development in the zebrafish. *Nat Med.* 2006;12:711-716.
12. Isogai S, Lawson ND, Torrealday S, Horiguchi M, Weinstein BM. Angiogenic network formation in the developing vertebrate trunk. *Development.* 2003;130:5281-5290.
13. Alders M, Hogan BM, Gjini E, Salehi F, Al-Gazali L, Hennekam EA, Holmberg EE, Mannens MMAM, Mulder MF, Offerhaus GJA, Prescott TE, Schroor EJ, Verheij JBGM, Witte M, Zwijnenburg PJ, Vikkula M, Schulte-Merker S, Hennekam RC. Mutations in *CCBE1* cause generalized lymph vessel dysplasia in humans. *Nat Gen.* 2009;41:1272-1274.
14. Hogan BM, Herpers R, Witte M, Helotera H, Alitalo K, Duckers HJ, Schulte-Merker S. Vegfc/Flt4 signalling is suppressed by Dll4 in developing zebrafish intersegmental arteries. *Development.* 2009;136:4001-4009.

15. Theodosiou A, Arhondakis S, Baumann M, Kossida S. Evolutionary scenarios of Notch proteins. *Mol Biol Evol.* 2009;26:1631-1640.

16. Geling A, Steiner H, Willem M, Bally-Cuif L, Haass C. A gamma-secretase inhibitor blocks Notch signaling in vivo and causes a severe neurogenic phenotype in zebrafish. *EMBO Rep.* 2002;3:688-694.

17. Hofmann JJ, Iruela-Arispe ML. Notch signaling in blood vessels: who is talking to whom about what? *Circ Res.* 2007;100:1556-1568.

18. Roca C, Adams RH. Regulation of vascular morphogenesis by Notch signaling. *Genes Dev.* 2007;21:2511-2524.

19. Sainson RC, Harris AL. Anti-Dll4 therapy: can we block tumour growth by increasing angiogenesis? *Trends Mol Med.* 2007;13:389-395.

20. Leslie JD, Ariza-McNaughton L, Bermange AL, McAdow R, Johnson SL, Lewis J. Endothelial signalling by the Notch ligand Delta-like 4 restricts angiogenesis. *Development.* 2007;134:839-844.

21. Phng LK, Gerhardt H. Angiogenesis: a team effort coordinated by notch. *Dev Cell.* 2009;16:196-208.

22. Swift MR, Weinstein BM. Arterial-venous specification during development. *Circ Res.* 2009;104:576-588.

23. Pendeville H, Winandy M, Manfroid I, Nivelles O, Motte P, Pasque V, Peers B, Struman I, Martial JA, Voz ML. Zebrafish Sox7 and Sox18 function together to control arterial-venous identity. *Dev Biol.* 2008;317:405-416.

24. Song HD, Sun XJ, Deng M, Zhang GW, Zhou Y, Wu XY, Sheng Y, Chen Y, Ruan Z, Jiang CL, Fan HY, Zon LI, Kanki JP, Liu TX, Look AT, Chen Z. Hematopoietic gene expression profile in zebrafish kidney marrow. *Proc Natl Acad Sci U S A.* 2004;101:16240-16245.

25. Holley SA, Julich D, Rauch GJ, Geisler R, Nusslein-Volhard C. her1 and the notch pathway function within the oscillator mechanism that regulates zebrafish somitogenesis. *Development.* 2002;129:1175-1183.

26. Riedel-Kruse IH, Muller C, Oates AC. Synchrony dynamics during initiation, failure, and rescue of the segmentation clock. *Science.* 2007;317:1911-1915.

27. Milan DJ, Giokas AC, Serluca FC, Peterson RT, MacRae CA. Notch1b and neuregulin are required for specification of central cardiac conduction tissue. *Development.* 2006;133:1125-1132.

28. Lorent K, Yeo SY, Oda T, Chandrasekharappa S, Chitnis A, Matthews RP, Pack M. Inhibition of Jagged-mediated Notch signaling disrupts zebrafish biliary development and generates multi-organ defects compatible with an Alagille syndrome phenocopy. *Development.* 2004;131:5753-5766.

29. Campbell WA, Yang H, Zetterberg H, Baulac S, Sears JA, Liu T, Wong ST, Zhong TP, Xia W. Zebrafish lacking Alzheimer presenilin enhancer 2 (Pen-2) demonstrate excessive p53-dependent apoptosis and neuronal loss. *J Neurochem.* 2006;96:1423-1440.

30. Ny A, Koch M, Schneider M, Neven E, Tong RT, Maity S, Fischer C, Plaisance S, Lambrechts D, Heligon C, Terclavers S, Ciesiolka M, Kalin R, Man WY, Senn I, Wyns S, Lupu F, Brandli A, Vleminckx K, Collen D, Dewerchin M, Conway EM, Moons L, Jain RK, Carmeliet P. A genetic Xenopus laevis tadpole model to study lymphangiogenesis. *Nat Med.* 2005;11:998-1004.
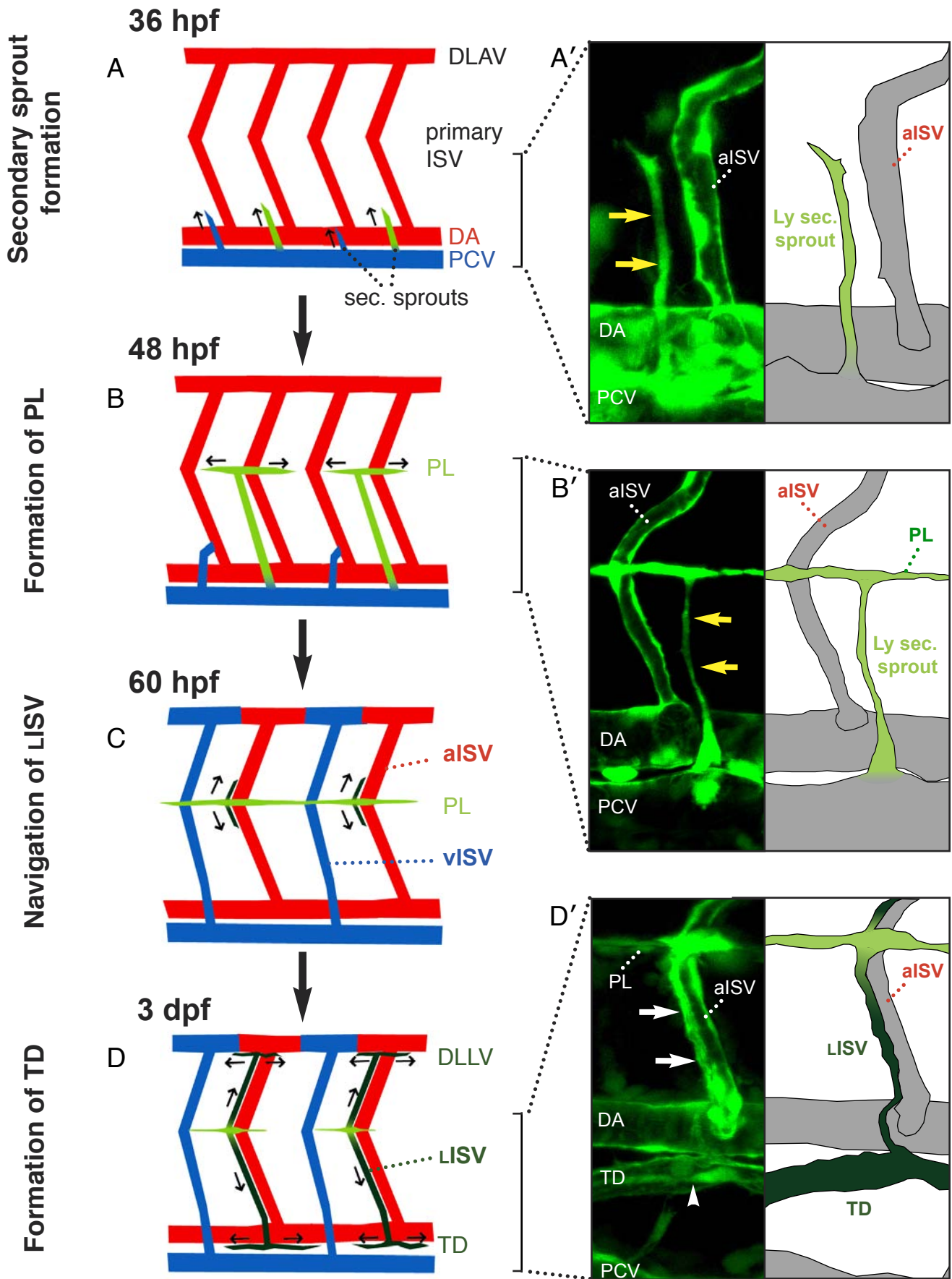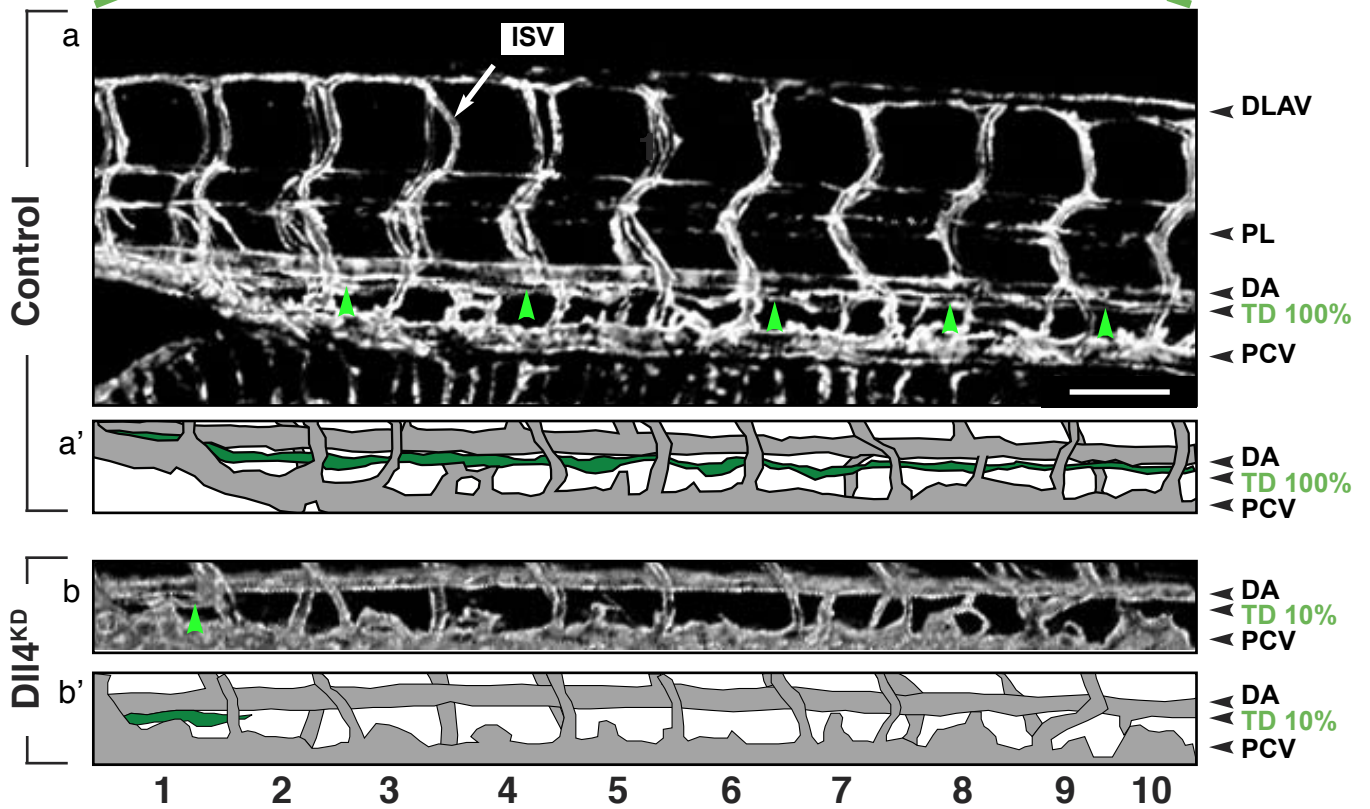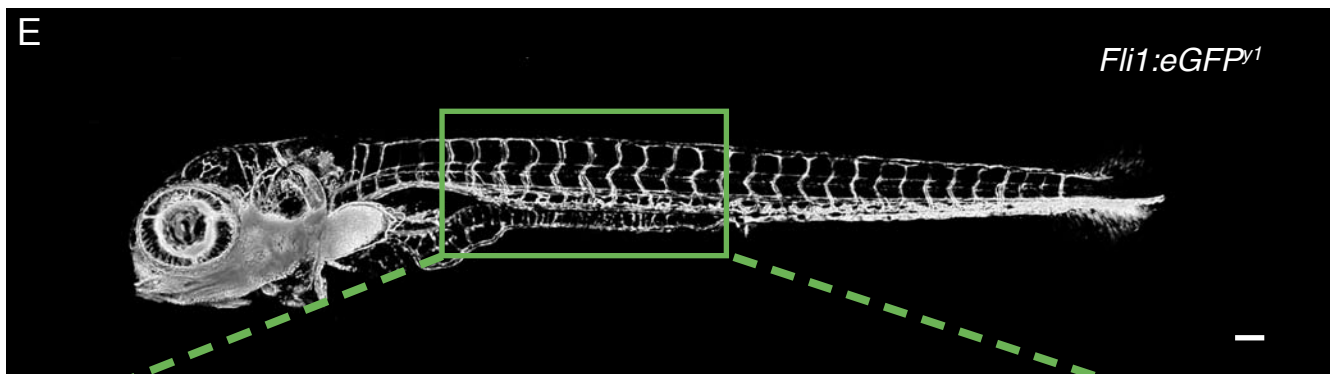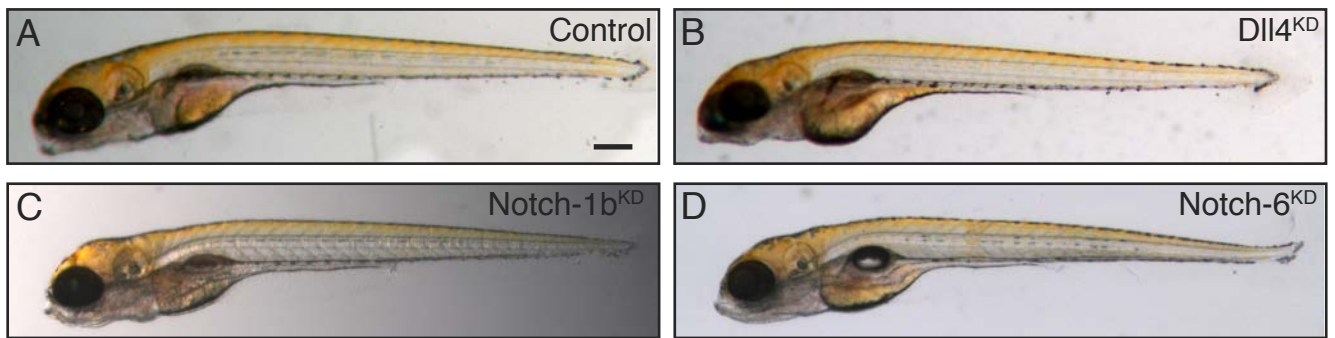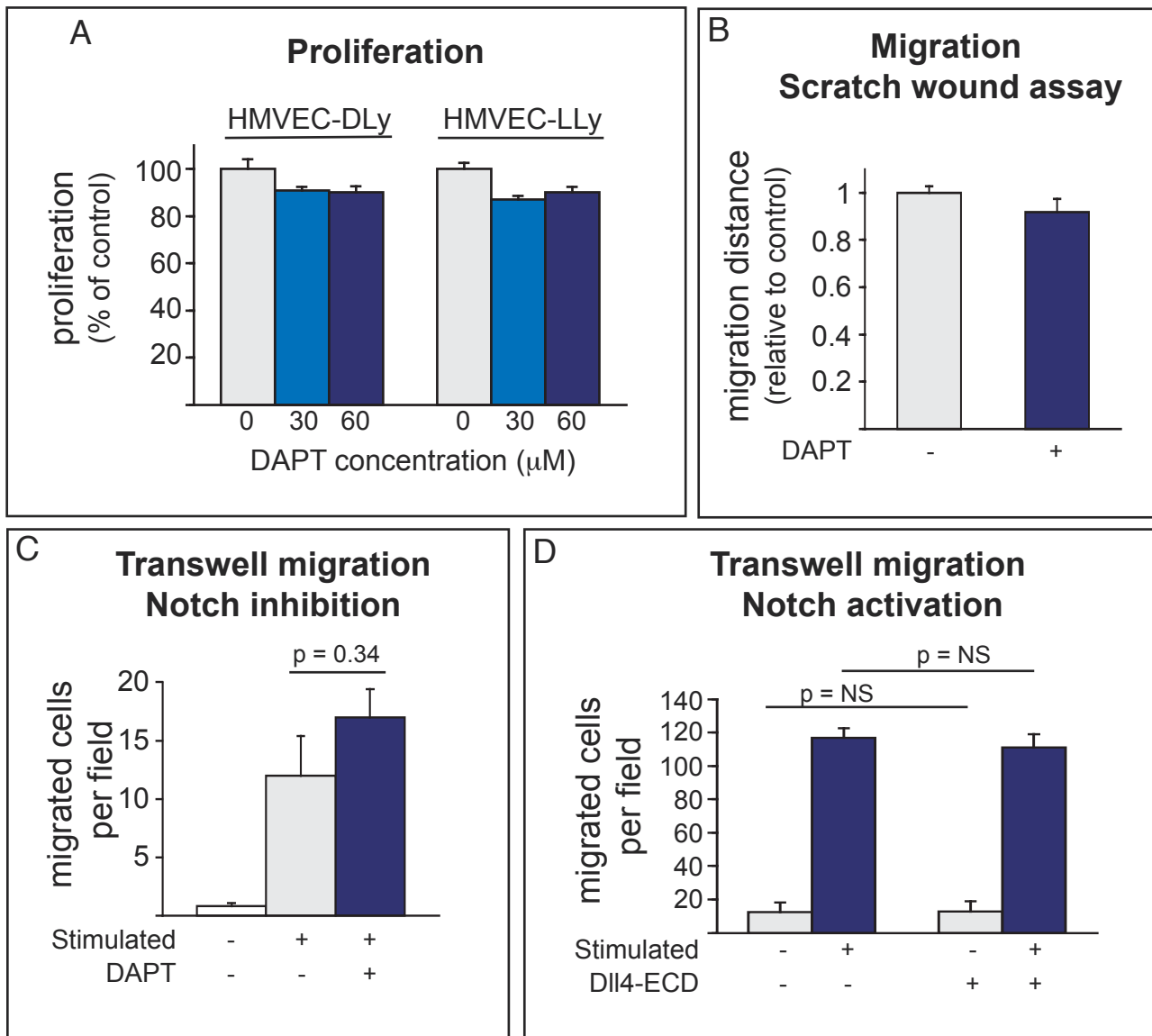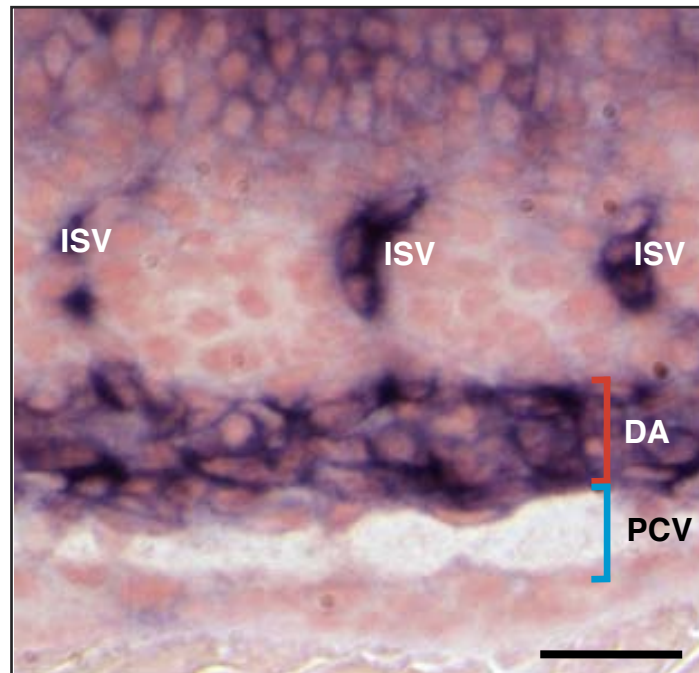
Supplemental Figure I

Supplemental Figure II

Supplemental Figure III

Supplemental Figure IV

A **Proliferation**

HMVEC-DLy   HMVEC-LLy

proliferation (% of control)

DAPT concentration (μM)

B **Migration Scratch wound assay**

migration distance (relative to control)

DAPT   -   +

C **Transwell migration Notch inhibition**

migrated cells per field

p = 0.34

Stimulated   -   +   +
DAPT   -   -   +

D **Transwell migration Notch activation**

migrated cells per field

p = NS

p = NS

Stimulated   -   +   -   +
Dll4-ECD   -   -   +   +
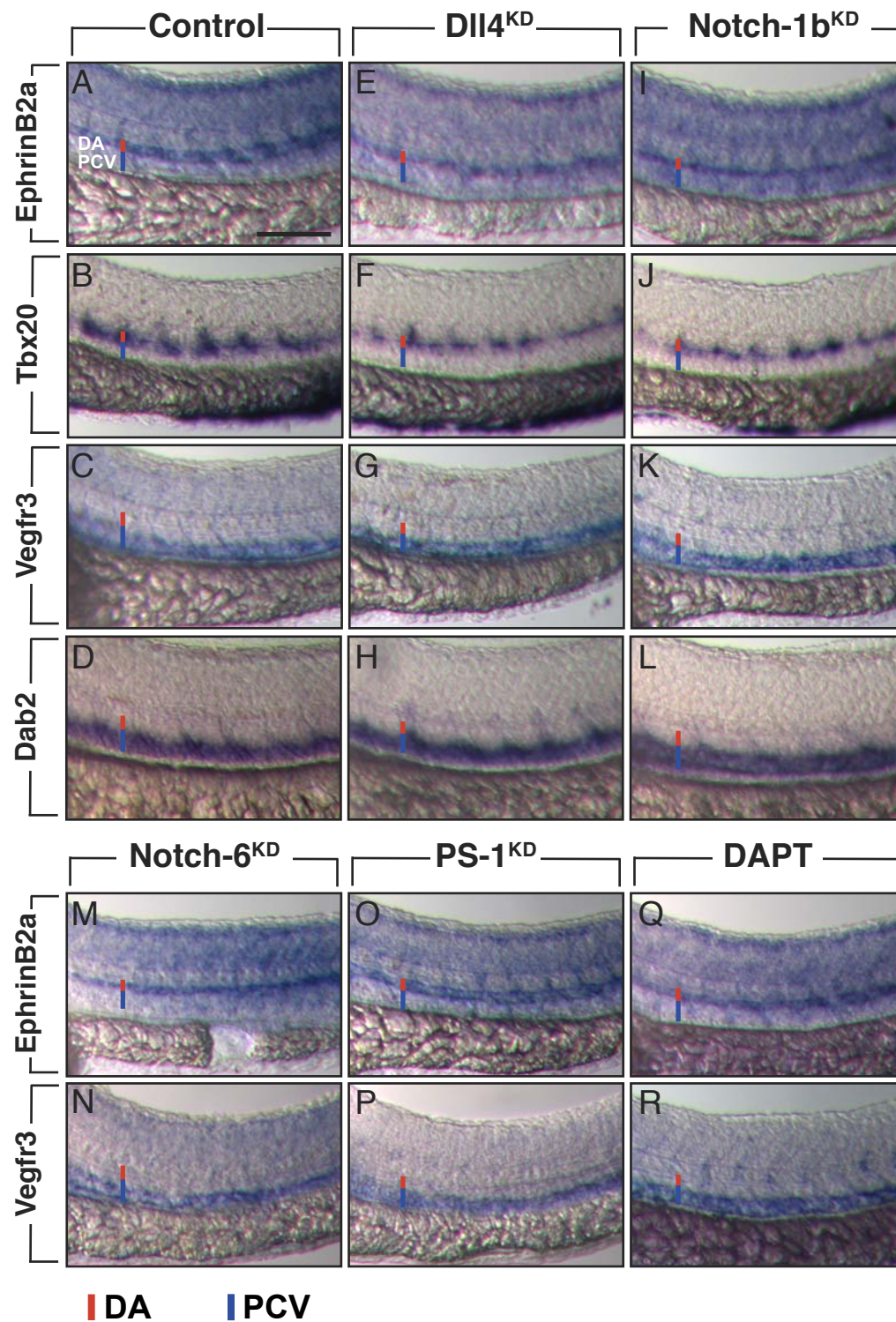
Supplemental Figure V

Supplemental Figure VI